TU Delft

Delft University of Technology

Document Version
Final published version

Licence
Dutch Copyright Act (Article 25fa)

Citation (APA)
Zhao, C., Zhang, X., Jin, Z., Yao, Z., Wagemaker, M., Li, H., Li, B., Huang, X., & Wang, Q. (2026). Chemical heterogeneity for battery materials. *Nature Reviews Chemistry*, *10*(6), 395-414. https://doi.org/10.1038/s41570-026-00821-y

Important note
To cite this publication, please use the final published version (if applicable).
Please check the document version above.

Copyright
In case the licence states “Dutch Copyright Act (Article 25fa)”, this publication was made available Green Open Access via the TU Delft Institutional Repository pursuant to Dutch Copyright Act (Article 25fa, the Taverne amendment). This provision does not affect copyright ownership.
Unless copyright is transferred by contract or statute, it remains with the copyright holder.

Sharing and reuse
Other than for strictly personal use, it is not permitted to download, forward or distribute the text or part of it, without the consent of the author(s) and/or copyright holder(s), unless the work is under an open content license such as Creative Commons.

Takedown policy
Please contact us and provide details if you believe this document breaches copyrights.
We will remove access to the work immediately and investigate your claim.

This work is downloaded from Delft University of Technology.

nature reviews chemistry

https://doi.org/10.1038/s41570-026-00821-y

Review article

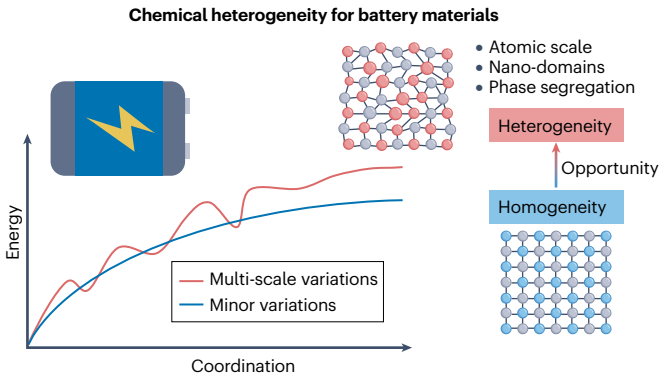
Check for updates

Chemical heterogeneity for battery materials

Chenglong Zhao[1,9], Xia Zhang[2,3,9], Zhou Jin[4], Zhenpeng Yao[5], Marnix Wagemaker[6], Hong Li[7] ✉, Baohua Li[8] ✉, Xuejie Huang[4,7] ✉ & Qidi Wang[2] ✉

Abstract

Next-generation rechargeable batteries require materials that offer enhanced electrochemical capabilities. Achieving these goals depends on understanding the fundamental principles governing these materials, which presents challenges associated to the complex interactions between composition, structural characteristics and electrochemical performance in battery materials. Despite intensive research, progress remains limited regarding effective strategies to mitigate the degradation of fragile alkali-metal-deficient frameworks arising from lattice stress and structural or chemo-mechanical instability upon cycling. In this Review, we explore the importance of chemical heterogeneity in rechargeable battery materials. We discuss how heterogeneity at atomic scale, nano-domains and up to phase-segregated levels within particles can enhance the electrochemical properties of battery materials beyond those of their homogeneous counterparts. Introducing chemical heterogeneity, principles and mechanisms can be unlocked to develop materials with improved structural stability, ion conductivity, redox activity, and phase transition characteristics, driving progress in battery technology. Finally, we outline the challenges and strategies for developing the future battery materials.



Sections

Introduction

Chemical heterogeneity of materials

Chemical heterogeneities and their effects on battery materials

Future challenges and outlook

Conclusions

A full list of affiliations appears at the end of the paper. ✉e-mail: hli@iphy.ac.cn; libh@mail.sz.tsinghua.edu.cn; xjhuang@iphy.ac.cn; wangqd@sustech.edu.cn

Introduction

Rechargeable batteries play an important role in energy storage and sustainability by powering various applications, ranging from portable electronics to electric vehicles, and emerging technologies, such as electric vertical-take-off and-landing aircraft[1,2]. Among various chemistries, alkali-metal-based compounds, particularly lithium (Li)-containing materials, represent the cornerstone of most battery systems to date[3–5]. Their utility stems from intercalation chemistry, according to which alkali ions reversibly insert into host lattices with minimal structural disruption[6–9]. This principle enables the use of structurally and compositionally homogeneous materials such as layered oxides (for example, $LiCoO_2$ (ref. 7)) and spinel oxides (for example, $LiMn_2O_4$ (ref. 10)), which offer predictable electrochemical behaviour owing to their well-defined atomic structures. Despite their apparent structural ideality, these materials are prone to degradation during cycling. For instance, in layered Li_xTMO_2 compounds (in which TM stands for transition metal), Li-ion extraction during charging reduces electrostatic shielding between adjacent TMO_2 slabs, resulting in slab gliding and stacking rearrangements, which can culminate in structural collapse[11–13]. These chemo-mechanical instabilities indicate a critical challenge: even structurally homogeneous, single-phase materials face intrinsic limitations under operational conditions. In response to the increasing demands for higher energy density and longer cycle life, continuous innovation in battery materials is imperative; this need has prompted a shift in battery materials research and design, moving beyond the pursuit of perfect homogeneity[14–18].

Historically, the evolution of materials science has long been shaped by the interplay between homogeneous and heterogeneous material design[19,20]. Homogeneous materials, characterized by uniform compositions and similar properties, provide predictable and reliable behaviours in terms of electrical, thermal and mechanical performances[21]. However, these materials also fall short when addressing the complex, multifaceted demands of modern applications[22,23]. This inherent constraint has driven the emergence of heterogeneous materials[24,25]. These materials, featuring multiple distinct phases or compositional variations at nanoscale to microscale dimensions, enable the integration of diverse functionalities that collectively surpass the capabilities of their homogeneous counterparts[26–28]. In the context of energy storage, heterogeneous materials, manifested as spatial variations in chemical composition, crystal structure or microstructure, could emerge as a potential strategy for enhancing their electrochemical performance[29–31]. Unlike conventional homogeneous battery materials, which often encounter trade-offs between energy density and cycle life, well-designed heterogeneous architectures could provide opportunities to balance multifaceted performances, thereby addressing these challenges in a more holistic manner.

The concept of heterogeneity in materials design can take inspiration from natural systems, in which multifunctionality often arises from structural and chemical complexity[32]. For instance, mineral paragenesis involves the coexistence of multiple minerals within a shared geological matrix, leading to improved mechanical strength and chemical resilience. Many synthetic battery materials, such as spinel $LiMn_2O_4$ (ref. 10), olivine $LiFePO_4$ (ref. 5) and garnet $Li_7La_3Zr_2O_{12}$ (ref. 33), are derived from natural mineral analogues and are synthesized under conditions that mimic natural mineral formation (such as high temperature, high pressure and gas atmospheres)[5,10,33,34]. These conditions naturally give rise to structural and chemical inhomogeneities[35,36], whether through incomplete phase transformation, elemental segregation or lattice defects. Rather than viewing these features as undesirable imperfections[37], such heterogeneities are increasingly recognized as designable features with the potential to improve electrochemical functionality. The resulting heterogeneous materials could therefore be defined by domains of substantial variation in properties, arising from differences in the microstructure, crystal structure or chemical composition[20,38,39]. These chemically distinct zones may span length scales from the atomic level to several micrometres or even millimetres, and they can assume a wide range of geometries and distributions. This inherent diversity introduces complex electrochemical behaviours, including reaction mechanisms, ion transport pathways, phase transition dynamics and strain evolution.

Studies have begun to explore how such 'chemical heterogeneity' affects key battery performance metrics. For example, localized variations in cation distribution can shift redox potentials or influence reaction kinetics[14,40,41], whereas compositional heterostructures can alleviate mechanical strain by redistributing stress fields[42,43]. Moreover, kinetically induced heterogeneities that evolve during battery operation can generate self-organized architectures that enhance reversibility[44–46]. However, the introduction of heterogeneity also brings new challenges, particularly in terms of synthesis complexity, structural characterization and mechanistic interpretation. A comprehensive understanding of how multiscale heterogeneities form and evolve, and how they influence electrochemical properties, is essential for expanding the design space and engineering structures that enable high-performance batteries.

In this Review, we focus on the emerging role of chemical heterogeneity in governing the fundamental properties of battery materials. We begin by discussing the incorporation of chemical heterogeneity in battery research and how it influences materials properties for enhanced electrochemical performance, in terms of ion transport, electrochemical reversibility, phase transitions, interfacial stability, energy and power density, and battery lifespan (Fig. 1). Specifically, we explore the various types of chemical heterogeneities present within individual particles of battery materials, ranging from short-range atomic distributions in several ångströms to nano-domains in several nanometres and phase segregation in micrometres, along with their reaction mechanisms. Additionally, beyond the thermodynamics-driven, we examine kinetics-induced heterogeneity that develops during cycling as a potential strategy to improve ion transport and structural robustness. Finally, we outline the challenges and opportunities associated with developing materials that feature both chemical and structural heterogeneities, aiming for a fundamental understanding and enhanced performance in this rapidly evolving field.

Chemical heterogeneity of materials

Within the conventional framework, which defines materials as structurally and compositionally uniform, heterogeneity has long been regarded as an undesirable deviation — a feature thought to compromise structural stability and degrade overall performance. However, as engineering demands increasingly require the integration of multiple, often conflicting, properties, the limitations of homogeneous materials have become more and more apparent[20]. A typical example is found in metallic systems such as nano-grained copper and aluminium. These metals, with grain sizes below 100 nm, can achieve strengths comparable with or exceeding those of high-strength steels[47,48]; however, they suffer from severely limited tensile ductility, in which once the load exceeds yield, catastrophic failure occurs with minimal plastic deformation[49,50]. This intrinsic trade-off between strength and ductility

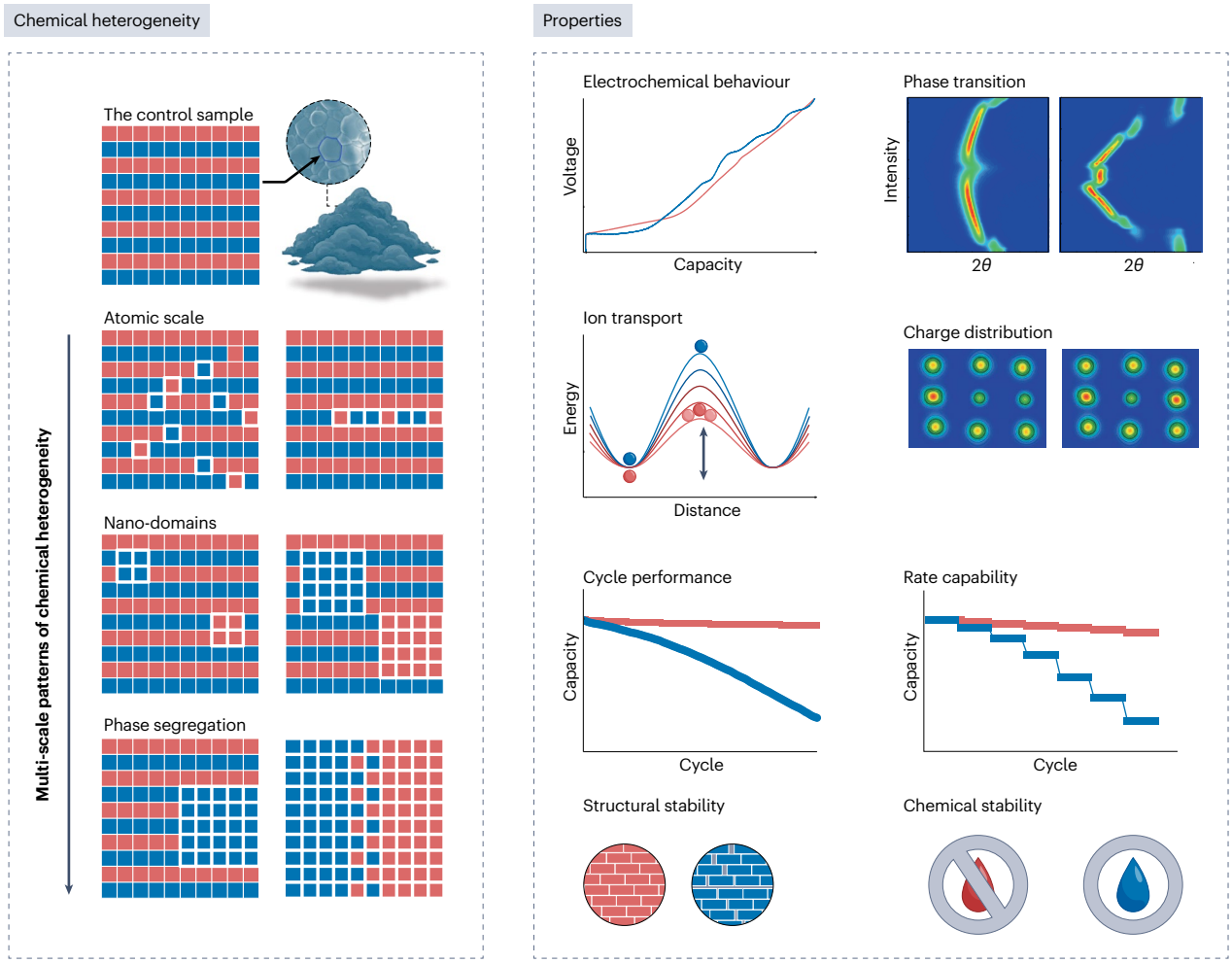


Fig. 1 | Categories of chemical heterogeneity and their effects on battery materials. Left panel, schematic highlighting the scale-dependent nature of chemical heterogeneity. At the atomic level, it appears as localized compositional fluctuations within the crystal lattice. As the scale increases (in the direction of the downward arrow), these fluctuations develop into nanoscale domains, and, at even larger scales, phase segregation and structural complexity emerge. Right panel, such multiscale heterogeneity can affect multiple aspects of battery materials, including electrochemical behaviour, phase transitions, ion transport, charge distribution, cycling stability, rate capability, and overall structural and chemical stability. These effects may occur in one or more of these areas simultaneously, influencing material performance in various aspects. The red curves show the performance of materials with chemical heterogeneity, while the blue curves show typical homogeneous materials. The diffraction patterns are representative only of what might be observed during a phase transition, but do not reflect actual data.

is a widely observed phenomenon in nanostructured metals and has long posed a critical obstacle to their broader application[51,52]. To address this dilemma, the intentional introduction of chemical heterogeneity has emerged as a promising strategy. In the case of nanocrystalline or ultrafine-grained metals, the design of heterostructures across multiple length scales, such as nano-domain architectures[53], dual-phase systems[49] and nano-twinned configurations[54], has enabled the simultaneous realization of high strength and improved ductility. Beyond structural metals, heterogeneity has transformative potential in diverse functional materials, including optoelectronics[55–57], thermoelectrics[58] and biomaterials[59,60]. In these systems, compositional variation engineering serves as an effective design principle to achieve synergistic property optimization, often enabling performance that would be difficult or impossible to attain in homogeneous materials. For instance, in thermoelectric materials, engineered multiphase heterostructures or nanoscale inclusions can effectively scatter mid-wavelength to long-wavelength phonons, reducing lattice thermal conductivity. At the same time, electronic transport may be preserved or even enhanced via energy filtering and carrier-mobility tuning, leading to an improved thermoelectric figure of merit[58]. These examples indicate that heterogeneity is not merely a tolerable defect but a widely applicable design model that enables the reconciliation of traditionally conflicting material properties through a controlled variation in structure and composition.

Given these advantages, the concept of chemical heterogeneity is particularly relevant to energy-storage systems, in which materials are subjected to coupled electrical, chemical, thermal and mechanical fields. The growing demand for fast ion transport, structural integrity and long-term cycling stability has exposed the limits of conventional homogeneous materials. By contrast, chemical heterogeneity offers

a pathway to spatially tailor material properties, especially within individual particles, by enabling localized control over key functional attributes of battery materials, as is discussed in the following sections.

Chemical heterogeneities and their effects on battery materials

Chemical heterogeneity, which emerges across multiple length scales during the synthesis and processing of battery materials, plays a pivotal role in governing the said materials' electrochemical performance. Here, we categorize it into four types based on spatial scale and origin: atomic-scale heterogeneity, nano-domain heterogeneity, phase segregation and kinetically induced heterogeneity arising from non-equilibrium ion transport and migration. These types span from the ångström to the micrometre scale. Importantly, this Review focuses on heterogeneity within individual particles, allowing us to isolate the effects of intrinsic, localized variations in composition and structure, without the added complexity of multi-material systems. We explore how their implications influence key electrochemical properties, including structural stability, ionic conductivity, interfacial behaviour and redox activity, for both electrodes and electrolytes. Particular attention is paid to kinetically induced heterogeneity, a distinct and important category, which often appears but is typically considered detrimental to material performance.

Chemical heterogeneity at the atomic scale

This subsection explores the role of atomic-scale chemical heterogeneity in designing high-performance electrode and electrolyte materials. At this scale, heterogeneity arises from the localized distribution of atoms within the crystal lattice, typically spanning only a few nearest-neighbour distances. These atomic-level variations give rise to local structural motifs that deviate from the average long-range crystal symmetry, forming different dimensions on the scale of several ångströms. These subtle yet critical features can have important effects to modulate phase transitions, enhance ionic conductivity, improve redox reversibility and facilitate ion diffusion. By intentionally introducing or controlling heterogeneity at this fundamental scale, it becomes possible to tailor the functional properties of battery materials for improved electrochemical performance.

Modulating phase transitions. Layered oxides have attracted considerable attention as cathode materials for Li-ion batteries, owing to their high energy density and well-defined layered structures that facilitate rapid ion diffusion. Among them, the O3-type layered oxides, characterized by octahedral alkali-metal coordination and an ABCABC oxygen-stacking sequence, represent a prototypical framework for high-performance cathodes[61]. A classic example is $LiCoO_2$, which crystallizes in a rhombohedral structure (space group *R*-3*m*) comprised of alternating Li and Co layers separated by close-packed oxygen planes[7]. Owing to its excellent electrochemical properties, $LiCoO_2$ has been extensively used in commercial Li-ion batteries. During electrochemical cycling, Li ions are reversibly extracted and reinserted into the lattice, a process accompanied by changes in the oxidation state of Co^{n+} and variations in lattice parameters. However, charging induces complex structural transformations that greatly affect long-term stability and performance[7,62]. At the initial stage of charging (~3.95 V), the *c*-axis lattice expands due to increased electrostatic repulsion between CoO_2 slabs, a process that remains largely reversible and structurally stable. Upon further charging to ~4.15 V (corresponding to $Li_{0.5}CoO_2$), a phase transition involving Li/vacancy ordering transforms the structure from hexagonal to monoclinic[62,63]. Continued delithiation in the 4.2–4.5 V range results in the formation of intermediate H1–H3 phases, characterized by staging phenomena and considerable lattice changes, introducing pronounced structural strain. Above 4.5 V, deep delithiation triggers more severe phase transitions towards monoclinic O1-type structures[64–66], often accompanied by oxygen loss and the formation of electrochemically inactive Co_3O_4. These irreversible changes degrade structural integrity and cause capacity fading, thereby limiting cycle life.

To mitigate these structural instabilities, an atomic-scale chemical heterogeneity, termed chemical short-range disorder, has been introduced as a design strategy. This was achieved through a rationally designed two-step synthesis process in which the $LiOH{\cdot}H_2O$ and $Co(OH)_2$ raw materials are first heated at 700 °C in air to form the Li/Co disordered structure and subsequently calcined at 1,000 °C in an oxygen atmosphere to form the final layered structure[14]. The resulting material retained local structural disorder, with ~2.6% of Co ions occupying Li-ion sites (Fig. 2a), forming distinct local atomic arrangements that deviate from the long-range average crystal structure. This localized heterogeneity modifies the local TM–O interactions and effectively suppresses unfavourable slab sliding and phase transitions typically observed during delithiation in conventional, homogeneous $LiCoO_2$. In particular, it eliminates Li/vacancy ordering and suppresses the O3-to-H(1–3) transition, thereby enhancing structural stability (Fig. 2b). Additionally, the altered local electronic environment contributes to improved electronic conductivity. Collectively, these effects lead to considerable improvements in Li-ion storage performance, particularly in terms of cycling stability and rate capability. Such atomic-scale heterogeneity has become a universal strategy for structure–property tuning, extending to complex systems like multi-principal element medium-entropy and high-entropy alloys[67–70], in which these atomic-level heterogeneities induce substantial changes in both mechanical and structural properties[71–73], underscoring the broader applicability of this design principle.

Improving reversibility. The development of cathode materials for Li-ion batteries has progressed rapidly in response to the increasing demand for higher energy density, lower cost and improved sustainability. Although $LiCoO_2$ set the benchmark for structural stability, its cost and supply risks spurred the adoption of high-Ni compositions such as $LiNiO_2$ and its derivatives of $LiNi_xMn_yCo_{1-x-y}O_2$ ($x \geq 0.8$)[74,75]. These materials offer higher theoretical capacities (~200–240 mAh g^{-1}) while substantially reducing the dependency on Co content, making them attractive for next-generation cathodes, especially in electric vehicles and large-scale energy-storage systems for both high energy density and cost-effectiveness[76].

Despite their great potential, these cathode materials face intrinsic challenges, particularly under high-voltage operation or near-full delithiation. The substantial volume changes during Li-ion insertion and extraction generate severe lattice strain, initiating microcracks and eventually causing particle pulverization, compromising structural integrity. Another critical problem is the occurrence of oxygen redox reactions at high states of charge, driven by Ni 3*d*–O 2*p* hybridization[77,78]. These reactions lead to oxygen release and electrolyte decomposition, which greatly increase the risk of thermal runaway and other safety hazards. In addition, these materials are prone to cation migration and irreversible structural degradation, including the migration of Ni^{2+} into the LiO_2 slabs and the formation of oxygen vacancies. These changes often result in irreversible phase transitions

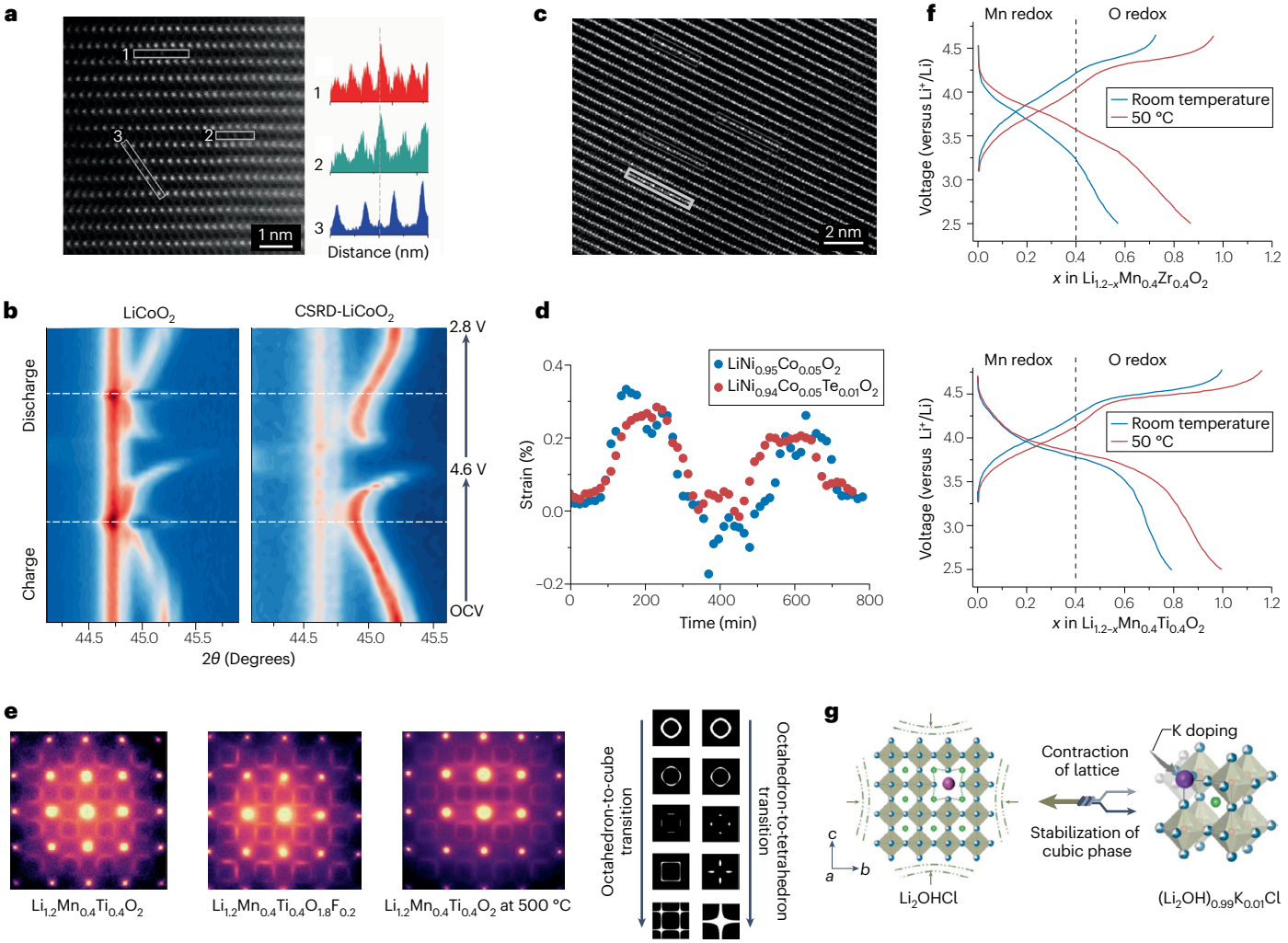


Fig. 2 | Chemical heterogeneity at the atomic scale. a, Crystal structure of chemical short-range disorder (CSRD)–$LiCoO_2$ material. Atomic-resolution high-angle annular dark-field scanning transmission electron microscopy (HAADF-STEM) image of the CSRD–$LiCoO_2$ material, together with line profiles along different crystallographic orientations. The white boxes indicate local variations in atomic distribution, revealing short-range compositional fluctuations within the lattice. **b**, In situ X-ray diffraction patterns of regular $LiCoO_2$ and CSRD–$LiCoO_2$ cathodes, demonstrating the phase evolution during electrochemical cycling. With nearly half of the Li ions removed, the cathode exhibits a clear Li^+/vacancy ordering phase transition from the hexagonal the monoclinic phase, resulting in the splitting of the reflections as indicated by the dashed lines. **c**, HAADF-STEM image of $LiNi_{0.94}Co_{0.05}Te_{0.01}O_2$ materials. **d**, The corresponding lattice strain maps highlighting local distortions derived from in situ X-ray diffraction. **e**, Electron diffraction patterns along the [001] zone axis for $Li_{1.2}Mn_{0.4}Ti_{0.4}O_2$, $Li_{1.2}Mn_{0.4}Ti_{0.4}O_{1.8}F_{0.2}$ and $Li_{1.2}Mn_{0.4}Ti_{0.4}O_2$ annealed at 500 °C, along with calculated diffraction locus corresponding to the octahedral-to-cubic and octahedral-to-tetrahedral short-range order transitions. **f**, Galvanostatic voltage profiles of $Li_{1.2}Mn_{0.4}Zr_{0.4}O_2$ and $Li_{1.2}Mn_{0.4}Ti_{0.4}O_2$ at elevated temperature and room temperature. The dashed lines denote the specific capacities based on Mn redox and O redox activity, respectively. **g**, Schematic illustration of lattice contraction and cubic-phase stabilization induced by K doping in Li_2OHCl, demonstrating how aliovalent substitution can facilitate ions diffusion. OCV, open-circuit voltage. Parts **a** and **b** adapted with permission from ref. 14, Springer Nature Limited. Parts **c** and **d** adapted with permission from ref. 40, Springer Nature Limited. Part **e** adapted with permission from ref. 41, CC BY 4.0. Part **f** adapted with permission from ref. 91, CC BY 4.0. Part **g** adapted with permission from ref. 104, CC BY 4.0.

from the original layered structure to spinel or rock-salt phases, leading to rapid capacity fading[79]. To mitigate such degradation pathways, various strategies have been explored, including surface coating[78,80], bulk doping[81–83] and compositional gradient architectures[84,85], aimed at stabilizing the crystal structure and enhancing long-term electrochemical performance.

One strategy involves the incorporation of trace Te^{6+} ions into $LiNi_{0.96}Co_{0.05}Te_{0.01}O_2$ to regulate the local atomic environment and improve structural reversibility. The presence of Te^{6+} promotes the formation of a thermodynamically stable Te–Ni–Ni–Te heterogeneous superstructure within the typically TM-disordered layered framework (Fig. 2c). This superstructure, derived from ordered Li_4NiTeO_6 layered oxide[86], strengthens metal–oxygen bonding and slightly enlarges inter-slab spacing, thereby alleviating lattice strain and suppressing cooperative lattice distortions under high-voltage operation (Fig. 2d). In parallel, the introduction of Te^{6+} also refines particle morphology, helping to mitigate the accumulation of mechanical stress, and preserves structural integrity. These synergistic effects, arising from

atomic-scale heterogeneity and morphology optimization, collectively contribute to improved phase transition reversibility and reduced mechanical degradation. As a result, the modified cathode exhibits high specific capacity and good cycling stability, showcasing the potential of atomic-scale heterogeneity as a design principle for advancing high-content Ni cathodes.

Activating oxygen redox reactivity. Cation-disordered rock salt (commonly abbreviated as DRX) cathodes have emerged as a promising class of materials for next-generation Li-ion batteries, owing to their capacity to activate both cationic and anionic (oxygen) redox reactions[87]. Unlike conventional layered cathodes, such materials exhibit a randomly distributed arrangement of Li and TM ions within a rock-salt (NaCl-type) lattice. This structure facilitates three-dimensional Li-ion transport and enables the incorporation of earth-abundant, low-cost elements such as Mn, reducing the dependence on critical metals such as Co and Ni[88,89]. A defining characteristic of DRX materials is their Li-rich composition, which creates local Li–O–Li configurations, suitable for triggering oxygen redox activity[90]. The participation of lattice oxygen in the redox process enables these cathodes to deliver high capacities, often exceeding 300 mAh g^{-1}. However, the use and reversibility of oxygen redox reactions are highly sensitive to atomic-scale structural features, particularly cation short-range order (SRO). Although DRX materials are globally disordered, they typically exhibit locally ordered SRO motifs, including tetrahedral, octahedral and cubic configurations[91]. These structural motifs define specific spatial correlations between cations and critically influence both Li-ion transport pathways and oxygen redox mechanisms[41]. For instance, the formation and connectivity of the '0-TM' channels (Li-ion migration pathways with zero adjacent TM ions) are essential for effective ion mobility and oxygen redox reactivity activation[87].

The tuneability of these local structures offers a potential design tool to optimize anionic redox reactivity. Through compositional engineering or thermal treatment, the nature and distribution of these motifs can be selectively modified[41] (Fig. 2e). For example, in $Li_{1.2}Mn_{0.4}Ti_{0.4}O_2$, the predominance of an octahedron-type structure correlates with the enhanced connectivity of Li-rich percolating networks and higher initial capacities. Fluorine-doping in $Li_{1.2}Mn_{0.4}Ti_{0.4}O_{1.8}F_{0.2}$ shifts the octahedron-type structure towards a cube-type structure, disrupting Li-ion migration pathways and reducing capacity. Annealing $Li_{1.2}Mn_{0.4}Ti_{0.4}O_2$ at 500 °C re-establishes the connectivity by inducing more extensive cube-type SRO with layered ordering, restoring the capacity beyond that of untreated or F-doped samples. These observations demonstrate that SRO-driven nanoscale heterogeneity directly affects both Li-ion transport and the activation of oxygen redox reactivity. Crucially, SRO also affects the reversibility and voltage efficiency of redox processes[91]. $Li_{1.2}Mn_{0.4}Ti_{0.4}O_2$, with relatively weaker local order and a higher density of 0-TM channels, enables deeper lithiation and exhibits reversible oxygen redox behaviour (Fig. 2f). By contrast, $Li_{1.2}Mn_{0.4}Zr_{0.4}O_2$, which possesses stronger cation ordering and fewer percolation pathways, displays sluggish oxygen redox activity, greater voltage hysteresis and diminished reversibility. Taken together, these results underscore the critical role of atomic-scale cation arrangements in shaping the oxygen coordination environment and determining the electrochemical accessibility of lattice oxygen. By tailoring local cationic heterogeneity, it becomes possible to activate and control oxygen redox reactions, thereby unlocking the capacity potential of these cathodes.

Facilitating ion diffusion. Inorganic solid electrolytes are central to all-solid-state battery development, offering advantages over liquid electrolytes such as improved safety, higher energy density and better thermal stability. However, their widespread adoption is often hindered by limited ionic conductivity and poor interfacial compatibility. Growing evidence indicates that the local crystal structure plays a pivotal role in governing ion transport behaviour[92–94]. By tuning the local coordination environment, lattice distortion and atomic-scale disorder, it is possible to create more favourable ion migration pathways and enhance structural dynamics, thereby boosting ionic conductivity[95]. Among various strategies, modifying the local coordination geometry of mobile ions has shown considerable promise. For instance, in $Li_3Zr_2Si_2PO_{12}$, inducing under-coordinated tetrahedral and pentahedral Li-ion sites enables three-dimensional diffusion pathways, greatly improving ion conductivity[96]. In $LiTi_2(PS_4)_3$, highly distorted Li sites introduce sublattice disorder and a frustrated energy landscape resembling that of liquids, resulting in superionic transport[97]. In garnet-type $Li_7La_3Zr_2O_{12}$, aliovalent doping creates additional vacancies and hopping sites, increasing room-temperature conductivity from ~10^{-6} S cm^{-1} in the undoped tetragonal $Li_7La_3Zr_2O_{12}$ to ~3.0×10^{-4} S cm^{-1} in its Al-doped or Ga-doped cubic counterpart[98,99].

An illustrative example of atomic-scale chemical heterogeneity is found in anti-perovskite electrolytes, which combine low-cost synthesis, good stability against Li metal and a low melting point (~300 °C) that enables scalable melt-infiltration processing[100,101]. However, their practical application is constrained by an inherently low ion conductivity. For instance, orthorhombic Li_2OHCl exhibits a conductivity of only 10^{-4}–10^{-5} mS cm^{-1} at 25 °C, which limits its effectiveness[102,103]. Partial substitution of $[Li_2OH]^+$ clusters with 1 mol% K ion induces an orthorhombic-to-cubic phase transition at room temperature (Fig. 2g). This structural transformation yields a more symmetric lattice, isotropic ion pathways and a contracted Li–O sublattice with enhanced orbital overlap, altogether reducing the activation energy for Li-ion migration[104]. The resulting material of $(Li_2OH)_{0.99}K_{0.01}Cl$ reaches an ionic conductivity of 4.5×10^{-3} mS cm^{-1} at 25 °C, nearly two orders of magnitude higher than the pristine compounds[102,103]. These examples, spanning coordination tuning, lattice distortion, phase transitions and defect engineering, demonstrate that atomic-scale structural features can be harnessed as a potential design principle. However, not all forms of atomic chemical heterogeneity are advantageous; when uncontrolled, they may induce parasitic effects that compromise electrochemical stability. By deliberately engineering local chemical environments, it is possible to mitigate such intrinsic limitations and fully unlock the electrochemical potential of solid electrolytes.

Chemical heterogeneity at nano-domains

As heterogeneity extends to the nanometre scale, variations within the nano-domains of individual particles become increasingly critical in determining the functional properties of battery materials. Compared with atomic-scale distortions, nanoscale features (such as partially ordered regions, single-layer domains and local compositional gradients) introduce larger structural motifs that greatly influence the thermodynamics and kinetics of Li-ion storage. These nanoscale heterogeneities can profoundly affect ion transport, redox activity, mechanical integrity and long-term cycling stability. Therefore, gaining a deeper understanding of nanoscale architectures, and achieving control over them, offers a promising route towards balancing high capacity with structural robustness, advancing the design of battery materials.

Increasing energy and power density. Owing to the abundance of Mn ore and its favourable redox characteristics, Mn-based DRX cathodes have emerged as attractive alternatives to conventional Ni-rich and Co-rich cathode materials[105]. These cathodes can deliver initial discharge capacities exceeding 300 mAh g^{-1}, primarily enabled by the electrochemical activity of the Mn^{3+}/Mn^{4+} and O^{2-}/O^{n-} redox couples[106]. However, involving oxygen redox processes often leads to structural instability within the face-centred cubic anionic framework, resulting in lattice degradation, voltage hysteresis and capacity fading upon cycling. To address these issues, incorporation of high-valent cations (such as Nb^{5+} and Ti^{4+})[107] and fluorine substitution[108] have been explored to stabilize low-valent Mn ions in the pristine state. This enables the use of the full Mn^{2+}/Mn^{4+} redox couple, thereby enhancing both capacity and reversibility while reducing the reliance on oxygen redox. For instance, materials such as $Li_2Mn_{2/3}Nb_{1/3}O_2F$ exhibit discharge capacities above 300 mAh g^{-1} with minimal oxygen evolution and suppressed voltage decay[109]. Despite these advances, conventional high-temperature solid-state synthesis often produces large, micrometre-sized particles, necessitating post-synthetic ball milling to improve performance[110,111]. Although this mechanical treatment can enhance capacity, it also introduces structural defects and unwanted phases[112], compromising cycling stability. In general, achieving high capacity in Li-rich materials requires particle sizes below 500 nm (ref. 113). For example, the capacity of $Li_{1.3}Mn_{0.4}Nb_{0.3}O_2$ drops sharply to only 100 mAh g^{-1} when the average particle size increases to the micrometre range[114].

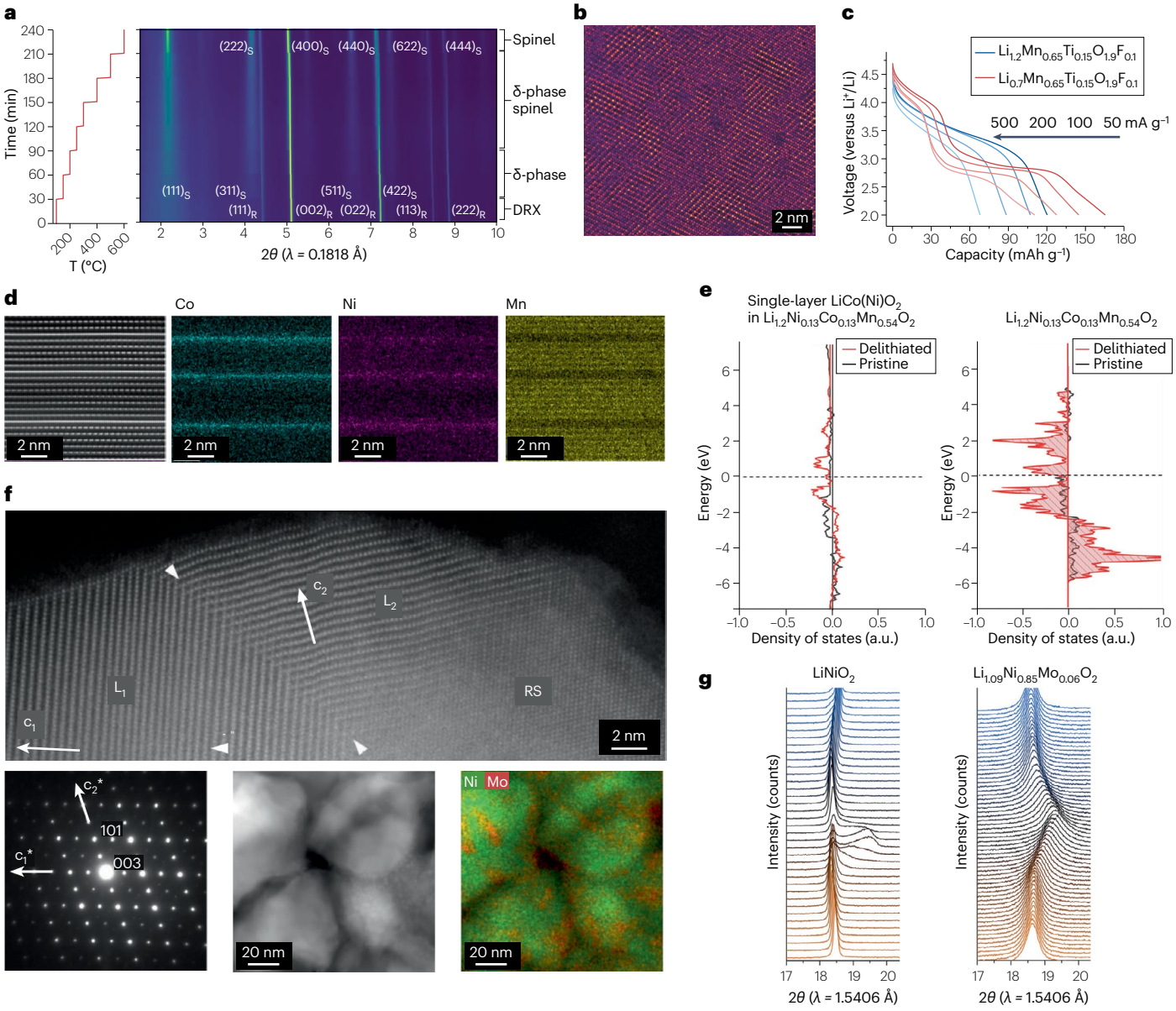
To circumvent this trade-off, introducing partially ordered spinel-like nano-domains through a two-step process, chemical delithiation followed by mild annealing at 200 °C (Fig. 3a), can substantially enhance capacity and rate capabilities without altering the particle size[115]. These nanoscale domains (3–7 nm in coherence length), embedded within the rock-salt matrix and separated by antiphase boundaries (Fig. 3b), inhibit long-range spinel ordering and suppress the undesirable two-phase lithiation reaction near 3 V, such as the transition between $LiMn_2O_4$ and $Li_2Mn_2O_4$ (refs. 116,117), which is typically associated with large volume changes and capacity degradation[118]. This engineered partially ordered spinel phase (δ-phase) microstructure enables relatively large particles (~5 µm) to achieve high capacity and improved rate capability (Fig. 3c), eliminating the need for nanosizing. Therefore, these environmentally benign, Li-rich materials with large particle sizes reduce the reliance on Co and Ni elements, thereby potentially improving energy density and enhancing safety. By contrast, the controlled materials generally require extended electrochemical activation to induce the formation of a spinel-like phase that provides three-dimensional Li-ion diffusion pathways[119,120]. Similarly, the strategy of introducing partially heterogeneous domains of varying sizes into a well-ordered crystalline structure has also proven effective in enhancing the fast-charging performance of anode materials[121,122].

Enhancing oxygen redox stability. Li-rich DRX materials exhibit high specific capacities, however, key challenges such as poor capacity retention and pronounced voltage hysteresis limit their practical viability. For example, $Li_{1.3}Mn_{0.4}Nb_{0.3}O_2$ shows rapid capacity fading, with discharge capacity dropping from 300 mA g^{-1} to 180 mAh g^{-1} within 20 cycles[123]. Although approaches such as surface coating[124] and fluorination strategies[125] have been explored to improve structural stability, their effectiveness remains limited, underscoring the need for further optimization. By contrast, Li-rich Mn-based layered oxides have attracted growing interest due to their better capacity retention. These materials typically feature an intergrowth structure in which rhombohedral $LiTMO_2$ and monoclinic Li_2MnO_3 phases exist in the same particles[123,126], enabling both cationic and anionic redox activity. In particular, the Li–O–Li configurations within the Li_2MnO_3 component generate non-bonding oxygen states that facilitate anion redox activity[90]. However, this activity also weakens the Mn–O bonds, increasing the risk of oxygen loss, structural degradation and voltage decay[127].

To mitigate these issues, an approach was developed involving the incorporation of single-layer disordered $LiCo(Ni)O_2$ nano-domains within the ordered Li_2MnO_3 matrix (Fig. 3d). This was achieved through a molten-salt ion-exchange process using a P2-type sodium (Na)-based precursors with a 2% LiOH excess as a reaction medium, which was calcinated at temperatures of 800 °C (ref. 42). The resulting $Li_{1.2}Ni_{0.13}Co_{0.13}Mn_{0.54}O_2$ composition exhibits synergistic functionality, in which the embedded heterogeneous disordered domains provide low-resistance pathways for Li-ion transport and divide the ordered matrix into nanoscale regions, effectively inhibiting long-range oxygen percolation and enhancing the stability of oxygen redox reactions[128]. The crystal orbital Hamilton population calculations reveal that these segregation layers strengthen metal–oxygen bonding and suppress the formation of oxygen–oxygen dimers (Fig. 3e), which are widely recognized as key contributors to voltage fade and Mn dissolution in Li-rich Mn-based layered oxides[129–132]. This intergrown heterogeneous architecture promotes fast Li-ion diffusion, reduces the domain size of the ordered phase and substantially improves the overall structural stability. Additionally, the uniformly dispersed configuration is considered more favourable, as it enhances the reversibility of lattice oxygen redox and mitigates voltage hysteresis[133].

Improving reversibility. Current efforts towards high-energy-density cathode materials primarily follow two main directions. The first centres on so-called Li-rich oxides ($Li_{1+x}TM_{1-x}O_2$), in which excess Li ions partially substitute TM ions within the TMO_2 slabs[134]. These materials can deliver exceptionally high capacities, largely attributed to anionic redox reactions involving non-bonding O 2*p* states[135,136]. However, they suffer from inherent drawbacks such as voltage hysteresis and voltage fade, primarily due to the instability of oxygen redox, which considerably hinders their practical viability unless these challenges are addressed[135]. The second route focuses on Ni-rich layered oxides, typically with Ni content exceeding 80%. Derivatives of $LiNiO_2$, these materials offer high capacities (>200 mAh g^{-1}) and elevated operating voltages (~3.8 V), making them promising candidates for commercial applications. However, they are plagued by mechanical degradation, phase transitions and thermal instability, particularly under high-voltage cycling conditions. To overcome these limitations, a hybrid strategy has emerged by integrating the Li-rich concept into Ni-rich layered oxides[43]. This approach takes advantage of the fact that introducing an excess of Li ions into the TMO_2 layers generates O 2*p* non-bonding states, which act as an additional redox reservoir, buffering the depletion of Ni–O hybridized states and thereby preserving the oxygen framework[137,138]. Moreover, partially replacing Ni^{3+} not only enhances theoretical capacity and reduces Ni content, mitigating associated stability issues, but also necessitates the introduction of high-valence, redox-inactive cations for charge compensation and structural reinforcement.

An example of this is $Li_{1.09}Ni_{0.85}Mo_{0.06}O_2$, in which excess Li ions and Mo^{6+} are incorporated into a $LiNiO_2$ matrix. Instead of forming a solid solution, Mo induces the formation of Li_4MoO_5 rock-salt nano-domains (~10 nm) that are coherently embedded within the layered matrix via



epitaxial interfaces[43] (Fig. 3f). This engineered nanoscale chemical heterogeneity effectively suppresses the phase transition between two hexagonal phases (H2–H3, specifically)[139], reduces lattice strain[140] and prevents microcrack formation during cycling[141]. In situ X-ray diffraction confirms that this material retains a highly reversible layered structure over extended voltage ranges (Fig. 3g), in contrast to undoped materials that undergo severe degradation. This intergrowth nanoscale heterogeneity endows Ni-rich layered cathodes

Fig. 3 | Chemical heterogeneity at nano-domains. a, In situ X-ray diffraction of $Li_{0.7}Mn_{0.65}Ti_{0.15}O_{1.9}F_{0.1}$ upon heating from 100 °C to 600 °C. During heating, a phase transition sequence is observed from cation-disordered rock salt (DRX) to a partially ordered spinel phase (*δ*) to an ordered spinel phase. The *δ*-phase is an intermediate phase between fully disordered rock-salt (R) and well-ordered spinel (S) compounds. **b**, Atomic-resolution high-angle annular dark-field scanning transmission electron microscopy (HAADF-STEM) image of *δ*-phase with $Li_{0.7}Mn_{0.65}Ti_{0.15}O_{1.9}F_{0.1}$ being chemically delithiated and subsequently heated at 200 °C for 2 h. **c**, Rate performance of $Li_{1.2}Mn_{0.65}Ti_{0.15}O_{1.9}F_{0.1}$ and *δ*-phase electrodes measured between 2 V and 4.8 V at 50 mA g^{-1}, 100 mA g^{-1}, 200 mA g^{-1} and 500 mA g^{-1}. **d**, HAADF-STEM image and atomic-resolution energy-dispersive spectroscopy mappings of the $Li_{1.2}Ni_{0.13}Co_{0.13}Mn_{0.54}O_2$ material with single-layer $LiCo(Ni)O_2$ structure. **e**, Crystal orbital Hamilton population calculations of O–O bond for $Li_{1.2}Ni_{0.13}Co_{0.13}Mn_{0.54}O_2$ and $Li_{1.2}Ni_{0.13}Co_{0.13}Mn_{0.54}O_2$ with single-layer $LiCo(Ni)O_2$ structure. The dashed line represents the Fermi level at 0 eV. **f**, HAADF-STEM image of the twinned domains of the layered *R*-3*m* structure (L_1 and L_2) along with a disordered rock-salt domain. The orientation of the *c*-axis in the layered domains is marked with arrows as c_1 and c_2. The (104) twin plane is traced with arrowheads. The electron diffraction pattern represents the twinned layered O3-type layered structure. The HAADF-STEM image and the colour-coded energy-dispersive spectroscopy map shows the mosaic Ni (green) and Mo (red) distribution. **g**, In situ X-ray diffraction patterns of $LiNiO_2$ and $Li_{1.09}Ni_{0.85}Mo_{0.06}O_2$ cathodes upon the H2–H3 phase transition. The peak shift appears low in magnitude in $Li_{1.09}Ni_{0.85}Mo_{0.06}O_2$ compared with that of $LiNiO_2$ because the bifurcation in the latter enables greater 2*θ* shift of the Li-poor phase. **h**, Scanning transmission X-ray microscopy images, the equilibrated structures and density profiles of poly(ethylene oxide) (PEO)/poly(vinylidene fluoride–hexafluoropropylene) (PVDF–HFP), poly(methyl methacrylate)/poly(vinylidene fluoride–hexafluoropropylene) (PMMA/PVDF-HFP) and poly(bis(trifluoroethoxy)phosphazene/poly(vinylidene fluoride–hexafluoropropylene) (PTFEP/PVDF-HFP) electrolytes. The density profile is plotted in the direction of the normal vector of the *x*-axis of the equilibrated cell and represents the concentration distribution of the constituents. Yellow is the bis(fluorosulfonyl)imide anion (FSI^-). Red is PEO/PMMA/PTFEP and green is PVDF-HFP. a.u., arbitrary units; λ, X-ray wavelength. H2 and H3 denote two hexagonal phases. Parts **a**–**c** adapted with permission from ref. 115, Springer Nature Limited. Parts **d** and **e** adapted with permission from ref. 42, Wiley. Parts **f** and **g** adapted with permission from ref. 43, The Royal Society of Chemistry. Part **h** adapted with permission from ref. 151, Springer Nature Limited.

with improved mechanical, structural and cycling stability, thereby expanding the design space for high-energy electrodes. Furthermore, incorporating other redox-inactive, high-valence cations such as W^{6+} and Zr^{4+} has shown similar benefits in simultaneously achieving charge compensation and lattice stabilization[82,142]. Notably, the incorporation of such high-valence cations requires precise control over sintering parameters and dopant levels. Improper processing may lead to the accumulation of these cations at grain boundaries or particle surfaces, resulting in a secondary-phase formation that disrupts electronic and ionic continuity, and compromises the structural integrity[143,144].

Facilitating ion diffusion. Solid polymer electrolytes have garnered increasing attention for solid-state batteries owing to their inherent interfacial compatibility with electrodes and ease of large-scale processing[145]. Structurally, most of these electrolytes consist of crystalline and amorphous domains[146,147] where the amorphous regions serve as the primary channels for Li-ion transport[148]. However, achieving high ionic conductivity, mechanical robustness and interfacial stability simultaneously remains challenging, as enhancing one property often compromises another. For instance, 'salt-in-polymer' systems suffer from poor salt dissociation and low conductivity, whereas 'polymer-in-salt' systems (though conductive) typically lack mechanical strength[149,150].

To address this trade-off, an approach involving the design of single-phase, locally high-concentration polymer electrolytes has been developed, which introduces a domain-level local heterogeneity while maintaining macroscopic structural uniformity[151]. In this architecture, ion-rich nano-domains are uniformly embedded within a mechanically robust polymer matrix, forming continuous Li-ion conduction pathways. This controlled heterogeneity not only improves conductivity but also promotes the in situ formation of a LiF-rich solid electrolyte interphase at the Li-metal interface, improving interfacial stability and suppressing dendrite growth[152]. Specifically, by blending a conductive polymer with a fluorinated, mechanically strong polymer, for instance, poly(bis(trifluoroethoxy)phosphazene) (PTFEP) with poly(vinylidene fluoride-co-hexafluoropropylene) (PVDF-HFP), a miscible, single-phase system can be constructed[151]. This avoids the formation of macroscopic phase boundaries that would otherwise hinder ion transport (Fig. 3h). As a result, by eliminating phase boundaries, this nanoscale heterogeneity enables the coexistence of high conductivity and mechanical strength, achieving simultaneous enhancement of both electrochemical performance and mechanical stability[153–155].

These advances in polymer electrolytes represent a broader theme in battery materials research: nano-domain engineering and chemical heterogeneity as a design model. From disordered rock salt and layered cathodes to locally structured polymer electrolytes, the strategic use of domain-level heterogeneity has proved effective in addressing key limitations, such as voltage hysteresis, poor rate capability, structural degradation and interfacial instability. This cross-cutting approach offers a potential pathway for the development of high-performance energy storage systems.

Chemical heterogeneity at phase segregation

As the scale of heterogeneity extends from the nanoscale to the microscale, increasing attention has been paid to phase segregation phenomena, particularly the integration of distinct phases or structural motifs within individual particles. Unlike atomic-scale or nanoscale variations, microscale heterogeneity introduces larger structural complexity that can have important effects on the performance and long-term stability of battery materials. Specifically, such phase segregation can improve mechanical integrity and modulate ion transport dynamics and interfacial stability during battery operation. This section focuses on the functional implications of microscale phase segregation, emphasizing how the deliberate integration of compositional or structural domains can be harnessed to mitigate degradation, improve kinetics and optimize electrochemical reversibility. By elucidating the underlying mechanisms and structure–function relationships, this discussion aims to offer new insights into the emerging role of controlled microscale heterogeneity in advancing high-performance battery materials.

Increasing energy and power density. In conventional ordered layered oxides, LiO_2 and TMO_2 slabs occupy alternating layers, forming a well-defined layered framework that enables rapid Li-ion diffusion through interlayer channels. By contrast, spinel-type oxides (despite sharing the same close-packed oxygen-anion framework) exhibit a distinct three-dimensional cation arrangement. For instance, in ideal $LiMn_2O_4$, Li ions occupy tetrahedral 8*a* sites whereas Mn ions reside in octahedral 16*d* sites, forming a three-dimensional percolating Li-ion

diffusion network[156]. Although this topology favours fast ion diffusion, this material suffers from limited practical capacity due to a first-order phase transition upon over-lithiation, leading to lattice reconstruction, stress accumulation and performance degradation[157].

To address these issues, a partially ordered spinel-phase regulation strategy has been reported, according to which, by tuning the local cation disorder and tailoring the anion framework, the electrochemical properties of spinel phases can be effectively optimized[158]. In the $Li_{1.47+x}Mn_{1.6}O_{3.4}F_{0.6}$ system, Li over-stoichiometry and fluorine incorporation are used to systematically control cation disorder via mechanochemical synthesis[159]. Substituting Mn with Li disrupts the fully ordered spinel lattice, forming a partially disordered rock-salt phase (Fig. 4a). However, excessive Li content can create unfavourable linear Li–O–Li configurations and elevate the average TM valence, promoting oxygen release and diminishing TM redox capacity[160,161]. Conversely, fluorination plays a stabilizing role by lowering the oxidation state of Mn and suppressing oxygen evolution, thereby enhancing both structural stability and energy density[109,162,163]. As a result, this engineered heterogeneity allows partially disordered spinel cathodes to access reversible oxygen redox, contributing to the capacity of a battery, while retaining partial spinel order to maintain continuous Li-ion transport pathways.

As cation disorder increases towards a fully disordered rock-salt configuration, oxygen redox activity becomes further activated.

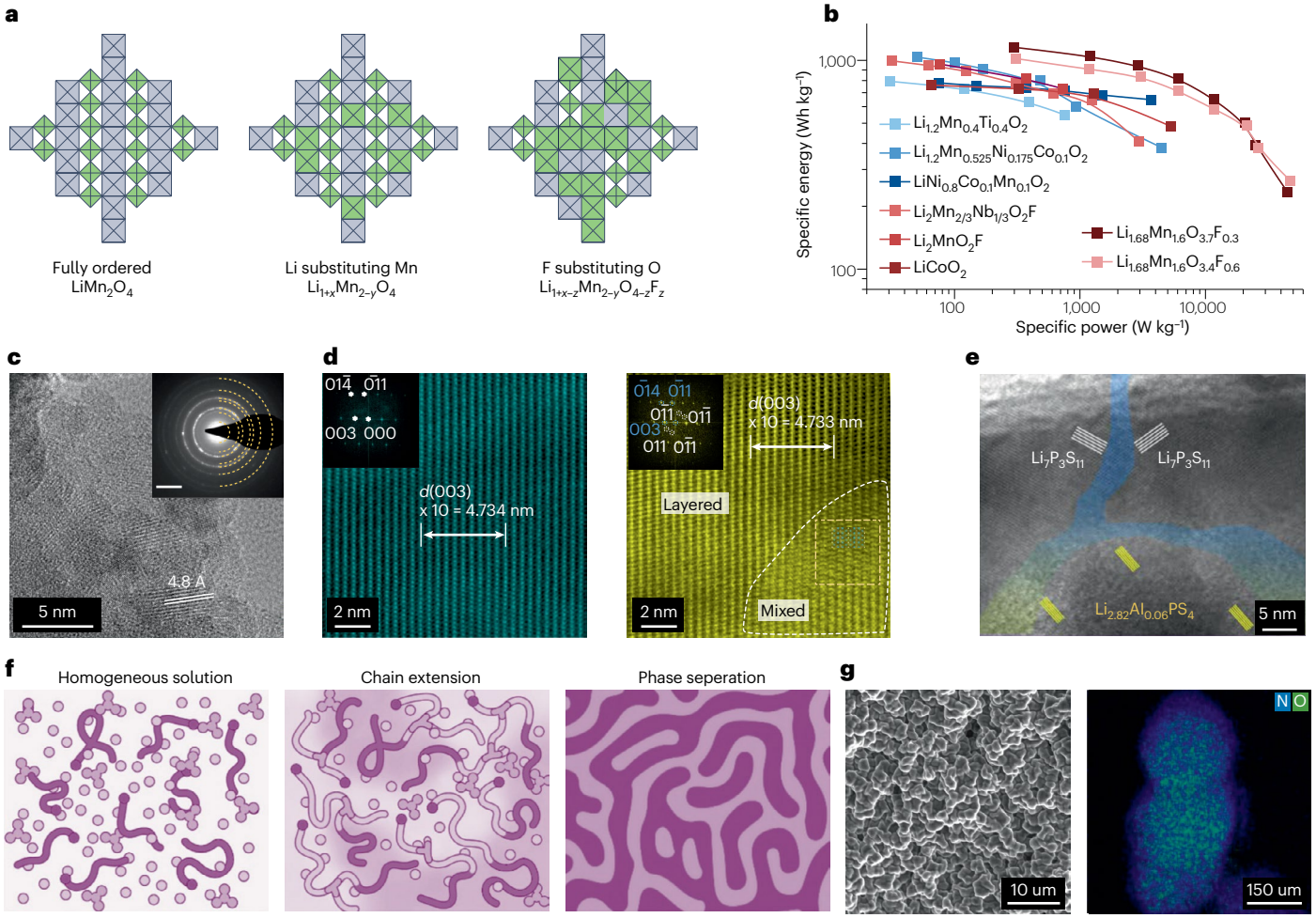


Fig. 4 | Chemical heterogeneity at phase segregations. a, Designing partially (dis)ordered spinel materials with Li over-stoichiometry, Mn substitution by Li and O substitution by F. The grey octahedra represent MnO_6; the green tetrahedra and octahedra represent LiO_4 and LiO_6, respectively. **b**, Ragone plot comparing the specific energy and power of $Li_{1.68}Mn_{1.6}O_{3.7}F_{0.3}$ and $Li_{1.68}Mn_{1.6}O_{3.4}F_{0.6}$ with those of state-of-the-art Li-ion cathodes with optimized rate performance as reported in the literature. **c**, High-resolution transmission electron microscopy (HRTEM) image of $Li_2Mn_{1.6}O_{3.7}F_{0.3}$. The inset shows the electron diffraction pattern of a partially ordered spinel lattice. **d**, Atomic-resolution high-angle annular dark-field scanning transmission electron microscopy images of $LiNi_{0.8}Co_{0.1}Mn_{0.1}O_2$ and La-$LiNi_{0.8}Co_{0.1}Mn_{0.1}O_2$. The insets show the corresponding fast Fourier transform of the images. The inset structure is the $La_4[LiMn]O_8$ phase with I_4/mmm symmetry. **e**, HRTEM image of $Li_7P_3S_{11}$–$Li_{2.82}Al_{0.06}PS_4$ electrolyte. **f**, Stepwise illustration of the polymerization-induced microphase separation process. **g**, Scanning electron microscopy image of plastic-crystal-embedded elastomer electrolyte, and electron energy-loss spectroscopy elemental mapping (N from the SN-based plastic crystal phase and O from the butyl acrylate-based elastomer matrix). Parts **a** and **c** adapted with permission from ref. 159, Elsevier. Part **b** adapted with permission from ref. 164, Springer Nature Limited. Part **d** adapted with permission from ref. 169, Springer Nature Limited. Part **e** adapted with permission from ref. 176, CC BY 4.0. Part **f** adapted with permission from ref. 188, Wiley. Part **g** adapted with permission from ref. 189, Springer Nature Limited.

Compositions such as $Li_{1.68}Mn_{1.6}O_{3.7}F_{0.3}$ and $Li_{1.68}Mn_{1.6}O_{3.4}F_{0.6}$ exhibit elevated specific energy and power densities[164], outperforming state-of-the-art commercial $LiCoO_2$ cathodes (Fig. 4b). This phase segregation strategy establishes a tuneable compositional space between fully ordered spinel and disordered rock salt (Fig. 4c), enabling the realization of high energy and power densities within a given system. These results exemplify how multi-scale heterogeneity, across atomic, structural and phase levels, can bridge key performance trade-offs, offering a compelling pathway for the development of energy-storage technologies. Notably, the concept of partially ordered structural phases shows broad applicability, extending to Na-ion cathodes, solid electrolytes[165] and even anode materials[166].

Increasing mechanical strength. Layered oxides, particularly Ni-rich materials, inherently experience considerable lattice strain during Li-ion insertion and extraction processes[13]. This strain arises primarily from two microscopic mechanisms[167,168]. First, the redox transitions of TMs (for instance, Ni^{3+} to Ni^{4+}) lead to a decrease in ionic radii, resulting in the contraction of [TMO_6] octahedra and a gradual reduction of the in-plane lattice parameter. Second, Li-ion extraction weakens interlayer electrostatic screening, enhancing repulsive O–O interactions and sharply changing the *c*-axis spacing. At high states of charge, these effects can culminate in structural collapse due to severe lattice destabilization. Upon cycling, such anisotropic lattice displacements accumulate, giving rise to internal lattice strain and inducing irreversible phase transitions. Conventional strategies aiming to synthesize defect-free, phase-pure materials often fail to alleviate these strain effects, especially in high-content Ni systems.

To address this issue, a potential heterostructure strategy has been proposed that introduces a strain-tolerant secondary phase to modulate lattice evolution during cycling[169]. Specifically, the integration of a coherent perovskite phase (La_4[LiTM]O_8) into $LiNi_{0.8}Co_{0.1}Mn_{0.1}O_2$ leads to the formation of a composite structure in which the perovskite functions as a structural rivet. This phase shares structural features with both layered and rock-salt frameworks and exhibits crystallographic compatibility with the host material. Owing to the closely matched lattice parameters, a coherent intergrowth is achieved, as confirmed by atomic-resolution HAADF-STEM imaging (Fig. 4d), resulting in a mechanically robust heterostructure. The coherent interface acts as a structural anchor, suppressing anisotropic lattice distortions during repeated cycles. Moreover, the high phase-transition barrier of the perovskite imparts a strong pinning effect, reducing cumulative strain and delaying detrimental structural transformations. As a result, the modified La-$LiNi_{0.8}Co_{0.1}Mn_{0.1}O_2$ demonstrates improved structural integrity and enhanced electrochemical durability. This approach represents an important advance towards zero-strain cathodes, in which a coherently integrated secondary phase enables strain regulation without compromising energy density, if the concentration of extracted Li ions can be controlled to be the same. Looking forward, this crystallographic interface engineering strategy could be extended to more complex rivet architectures, such as composite perovskites[170] or P2-type/O3-type intergrowth layered materials[171], opening new avenues for stabilizing advanced layered oxides under demanding operating conditions.

Facilitating ion transport. Sulfide-based glass ceramics have attracted substantial attention as solid electrolytes for the large-scale deployment of all-solid-state batteries, owing to their simple chemical composition, mild synthesis conditions and compatibility with scalable solid-state reactions. However, their practical implementation remains limited by their inherently low Li-ion conductivity at room temperature, especially in the absence of effective microstructural engineering strategies. Ion transport in these materials is highly sensitive to the microstructure of embedded crystallites, including grain boundaries, grain size, morphology and spatial distribution[172,173]. A classic example illustrating the role of interface engineering in ion conductors is the AgI and Al_2O_3 heterogeneous system, in which considerably enhanced Ag-ion conductivity is observed at the interface compared with the bulk phase[174,175]. This highlights the critical role of grain boundary design in enhancing ionic transport within solid electrolytes.

A nucleation-controlled strategy based on sequential crystallization and heterogeneous growth has been studied in the Li_2S–P_2S_5 system[176]. Specifically, the addition of Al_2S_3 as a nucleation promoter reduces the energy barrier for the formation of $Li_{2.82}Al_{0.06}PS_4$, which serves as a crystalline core. Subsequently, $Li_7P_3S_{11}$ nucleates and grows heterogeneously on the surface of $Li_{2.82}Al_{0.06}PS_4$ with diverse orientations, suppressing bulk crystal coalescence and yielding a spatial distribution of nano-hetero-domains. These domains are enriched with grain boundaries (Fig. 4e), which act as continuous, low-resistance channels for Li-ion transport. As a result, the $Li_7P_3S_{11}$–$Li_{2.82}Al_{0.06}PS_4$ heterostructure achieves an impressive room-temperature ionic conductivity of 13.2 mS cm^{-1}. This phase-scale heterostructure approach demonstrates broad versatility, as a range of nucleation accelerants, such as Ga_2S_3 and SiS_2, can be used to tailor crystallization behaviour. More broadly, this approach offers a general and scalable framework for constructing multiphase, grain-boundary-rich composite electrolytes, with substantial potential for extension to oxide-based and halide-based solid electrolytes[177,178]. By leveraging microstructural heterogeneity and phase-interface engineering, this opens new avenues for the rational design of high-performance solid electrolytes suitable for energy-dense and durable solid-state battery systems.

Improving interfacial stability. The commercialization of Li-metal batteries is critically constrained by persistent issues associated with the Li-metal anode, including uncontrolled dendrite growth, accumulation of electrochemically inactive Li[179], large volume fluctuations and formation of an unstable solid electrolyte interphase, all of which undermine safety, cycle life and reliability[180]. Solid polymer electrolytes have attracted increasing interest due to their mechanical flexibility, interfacial adaptability and compatibility with roll-to-roll manufacturing, making them promising candidates for practical solid-state Li-metal batteries[181,182]. However, conventional poly(ethylene oxide)-based electrolytes suffer from low ionic conductivity and limited interfacial stability, limiting their applicability[183]. Although approaches such as inorganic fillers, gel formation and hybridization have been explored, their performance improvements remain modest[184].

A possible approach to overcome these limitations is polymerization-induced phase separation, which enables the formation of interconnected, ion-conducting nanostructures embedded within a mechanically robust matrix[185,186]. Specifically, in the initial stage, two polymer blocks (typically such as polylactide or poly(ethylene oxide) and a copolymer formed from functional monomers and crosslinkers) form a homogeneous mixture[187]. As polymerization proceeds, the chain extension increases, and the incompatibility between the two blocks drives the formation of disordered nanoscale domains, marking the onset of microphase separation. Crosslinking kinetically arrests the structure in a disordered nanophase-separated state in which ion-conductive domains coexist with a mechanically

supportive matrix. With further chain growth or enhanced segmental incompatibility, the system may evolve into periodic morphologies such as lamellae, cylinders or gyroids (Fig. 4f). In particular, the intermediate disordered state stabilized by cross-linking offers a favourable balance between conductivity and mechanical strength, owing to its continuous transport pathways and tuneable domain sizes[188].

When integrated into a polymer electrolyte design, this approach can simultaneously improve ionic conductivity, mechanical resilience and electrode–interface compatibility. In situ polymerization during cell assembly facilitates the formation of a three-dimensional ion-conductive plastic crystal network within an elastomeric matrix[189]. This elastomeric scaffold conforms intimately to electrode surface features (Fig. 4g), minimizing interfacial voids and stress accumulation, thereby suppressing dendrite growth and enhancing interfacial stability.

These discussions indicate that the design of controlled phase separation is not limited to electrodes or electrolytes. Similar principles have been successfully applied across battery components, for example, introducing cation disorder into spinel cathodes, embedding coherent perovskite phases into layered oxides and engineering multiphase domains in sulfide-based solid electrolytes. However, it should be emphasized that uncontrolled and parasitic phase segregation, arising from local redox reactions, lattice instability or a kinetic imbalance, often leads to performance degradation in rechargeable batteries. For instance, in spinel $LiMn_2O_4$ and olivine $LiFePO_4$, the limited phase-boundary mobility can induce structural or kinetic phase segregation, resulting in capacity fading and poor cycling stability[128,190]. Therefore, when using phase-segregation-guided design strategies to optimize electrode architectures, it is crucial to carefully consider these potential side effects and to avoid unintended heterogeneity or local structural instability that could compromise electrochemical performance.

Kinetics-induced chemical heterogeneity

Beyond the thermodynamically driven chemical heterogeneity discussed previously, this section focuses on kinetically induced heterogeneity, which arises from non-equilibrium ion transport and migration within individual particles upon cycling. Traditionally, the construction of heterostructures has relied on synthesis or mechanical ball-milling, which offer limited control over the local composition and often fail to produce metastable or non-equilibrium structures with tailored functionalities. By contrast, electrochemical cycling, typically regarded as a means for performance evaluation, can itself serve as an unconventional synthetic route, inducing the formation of unique structural motifs and chemical domains that are inaccessible via conventional processing. This kinetics-induced chemical heterogeneity has been shown to play a critical role in improving ion transport kinetics, which is particularly valuable for fast-charging applications, substantially contributing to structural stabilization by relieving local strain, redistributing stress and suppressing detrimental phase transitions during cycling.

Facilitating ion diffusion. With the growing demand for cost-effective and scalable energy storage, Na-ion batteries have emerged as a potential alternative to Li-ion systems. A key challenge, however, lies in identifying safe and stable anode materials. Among available candidates, hard carbon is commonly used owing to its relatively high charge capacity. However, it operates at voltages very close to that of metallic Na, substantially increasing the risk of Na-metal plating and dendrite formation, posing serious safety hazards. By contrast, $Li_4Ti_5O_{12}$ stores Na ions at a considerably higher average voltage (~0.91 V versus Na^+/Na)[191], thereby reducing the risk of dendrite formation and offering a safer electrochemical profile. Remarkably, despite the substantial difference in ionic radii (Na ion, 1.02 Å and Li ion, 0.76 Å), the $Li_4Ti_5O_{12}$ spinel structure can reversibly accommodate both ions[192–194], underscoring its structural tolerance.

Although, owing to their larger size, Na ions generally exhibit higher migration barriers and slower diffusion kinetics than Li ions, their insertion into $Li_4Ti_5O_{12}$ induces a three-phase coexistence, namely coexistence of $Li_4Ti_5O_{12}$, $Li_7Ti_5O_{12}$ and $Na_6LiTi_5O_{12}$, which unexpectedly opens additional diffusion pathways and enhances Na-ion transport[195] (Fig. 5a). Notably, this phase transformation occurs heterogeneously within individual particles, with only partial regions undergoing structural reorganization. This localization of strain helps to mitigate the mechanical degradation typically associated with volume expansion during cycling. These findings challenge the long-standing view that spinel-type electrodes are unsuitable for Na-ion storage and instead reveal a distinct three-phase separation mechanism[196,197]. Beyond improving Na-ion anodes, this kinetics-induced chemical heterogeneity offers new insights into ion insertion chemistry, advancing the understanding of structure–function relationships in various systems[198–200].

Increasing energy and power density. As previously discussed, spinel-like domains can be engineered into Mn-based DRX oxides to enhance Li-ion transport kinetics. However, beyond synthetic control, electrochemical cycling itself can induce in situ spinel-like transformations, serving as a beneficial structural evolution pathway that improves electrochemical performance. In fluorinated materials, such as $Li_{1.2}Ti_{0.2}Mn_{0.6}O_{1.8}F_{0.2}$, prolonged cycling triggers a localized, gradual transformation from the disordered rock-salt phase towards a spinel-like configuration (Fig. 5b). This transformation, observed after tens of cycles, involves progressive structural reconstruction while retaining the overall disordered matrix[111]. Notably, rather than causing degradation, this evolution enhances electrochemical performance (Fig. 5c), as reflected by the emergence and extension of voltage plateaux around 3.0 V, characteristic of spinel-like phases that facilitate Mn-ion redox activation and faster Li-ion diffusion[201].

A similar phenomenon is observed in $Li_{1.1}Mn_{0.8}Ti_{0.1}O_{1.9}F_{0.1}$, in which cycling induces two distinct structural transformations. At high voltages, the coexistence of Mn^{4+} and Li-ion vacancies promotes local cation ordering, driving the formation of a spinel-like phase. At low voltages, Li-ion insertion and Mn^{4+} reduction lead to a partially ordered rock-salt phase structurally analogous to monoclinic β-$LiFeO_2$ (ref. 119). Together, these observations reveal a beneficial rock-salt-to-spinel transformation in oxides. Far from being a detrimental side reaction, the cycling-induced structural evolution can be strategically leveraged to unlock high capacities and improved stability in Co-free and Ni-free cathodes. As such, electrochemical cycling, traditionally viewed as a testing process, can also act as a dynamic tool for structural reconfiguration, enabling the in situ discovery of electrode chemistries.

Improving reversibility. Some oxide electrodes (such as CoO and FeO) undergo conversion reactions during lithiation, forming metallic nanoparticles dispersed in Li_2O matrices[202,203]. By contrast, intercalation-type materials accommodate Li ions within their lattice without disrupting their structures. However, even in such systems, local bonding environments may be perturbed, leading to partial structural reorganization. By controlling the depth of lithiation, it is possible

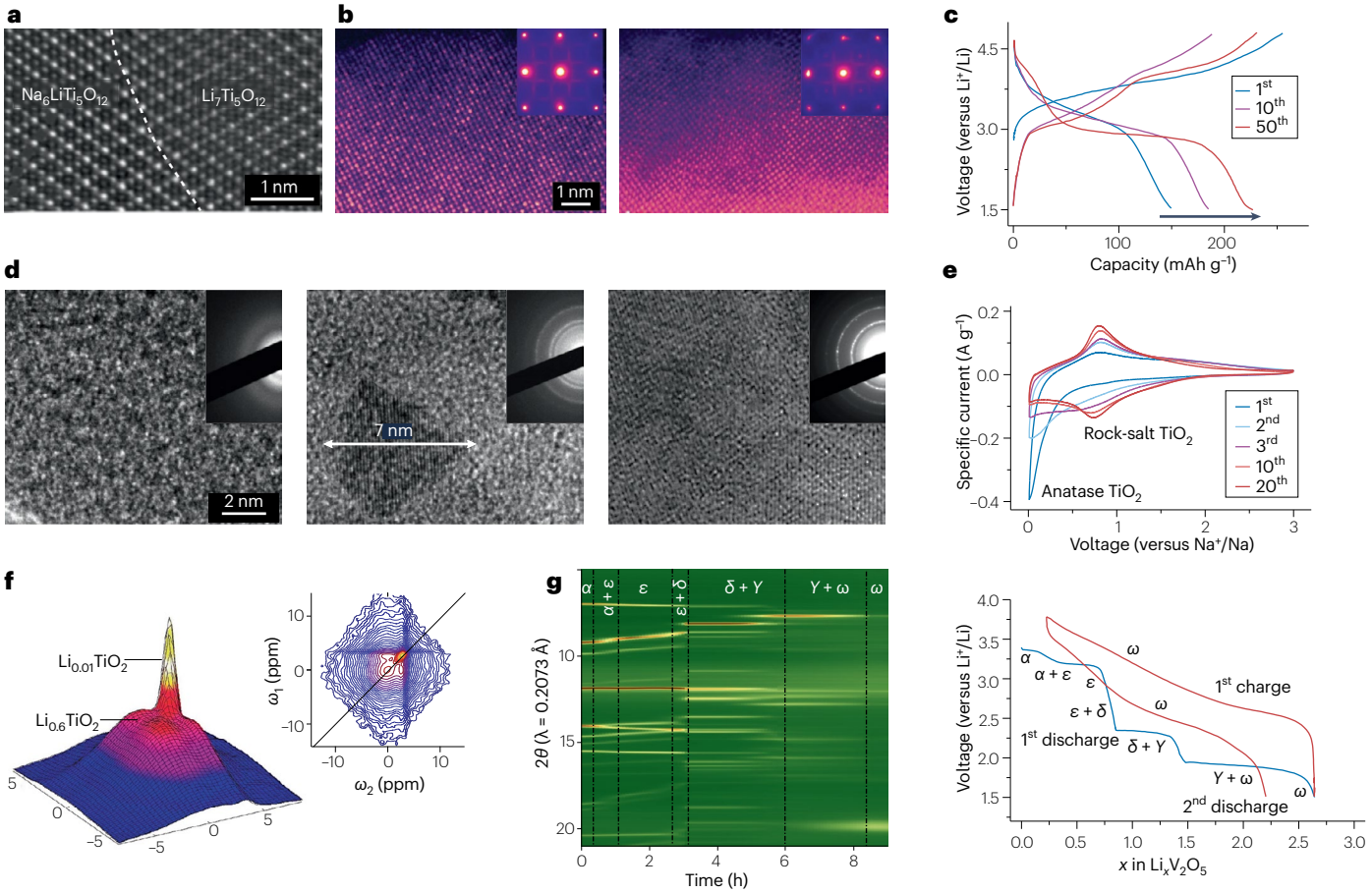


Fig. 5 | Kinetics-induced chemical heterogeneity. a, High-angle annular dark-field scanning transmission electron microscopy (HAADF-STEM) image of fully discharged $Li_4Ti_5O_{12}$ in Na cell. The coexistence of the two final phases, $Li_7Ti_5O_{12}$ and $Na_6LiTi_5O_{12}$, is identified with a phase boundary. **b**, Atomic-resolution HAADF-STEM images of a nanoscale region in pristine $Li_{1.2}Ti_{0.2}Mn_{0.6}O_{1.8}F_{0.2}$ (left) and the sample after 50 cycles (right). The insets show the corresponding electron diffraction patterns. **c**, Charge and discharge voltage profiles of $Li_{1.2}Ti_{0.2}Mn_{0.6}O_{1.8}F_{0.2}$ cathode. **d**, High-resolution transmission electron microscopy images of the samples in the pristine state (left), after the first cycle (centre) and after the 20th cycle (right). The insets show the electron diffraction patterns. **e**, Cyclic voltammetry curves of the anatase TiO_2 electrode for the initial 20 cycles at 0.2 mV s^{-1}, indicating multistep phase transformations from crystalline anatase to amorphous and then partial rock-salt $NaTiO_2$ compounds upon repeated cycling. **f**, ^{7}Li two-dimensional exchange between the two coexisting phases in $Li_{0.12}TiO_2$ material measured at T = 373 K and t_{mix} = 50 ms. Here, t_{mix} denotes the mixing time, that is, the time interval between the two measurements during which Li exchange occurs between the two coexisting phases. The contour plots (inset) are projections of the three-dimensional representations; ω_1 and ω_2 represent the chemical shift before and after t_{mix}. The cross-signal intensities are a direct measure of cross-boundary Li diffusion. **g**, In situ X-ray diffraction data collected during discharge and charge cycling of an α-V_2O_5 electrode in Li cell and the corresponding discharge and charge voltage profiles as it transitions through various phases (ε, δ, γ and ω). Part **a** adapted with permission from ref. 195, Springer Nature Limited. Parts **b** and **c** adapted with permission from ref. 46, Wiley. Part **d** adapted with permission from ref. 44, Springer Nature Limited. Part **e** adapted with permission from ref. 45, CC BY 4.0. Part **f** adapted with permission from ref. 206, Springer Nature Limited. Part **g** adapted with permission from ref. 211, American Chemical Society.

to selectively activate beneficial structural transformations, thereby enhancing the overall electrochemical performance. For instance, in amorphous Nb_2O_5, tuning the lithiation to incorporate three Li ions per formula unit triggers a spontaneous transformation into a rock-salt structure[44] (Fig. 5d). This new phase exhibits both high capacity and lower Li-ion diffusion barriers. Although the first cycle often introduces mechanical stress, driven by nucleation barriers or lattice distortions within the structural host[204,205], the voltage hysteresis diminishes upon cycling, indicating improved thermodynamic and kinetic reversibility.

A similar phenomenon is observed in Ti-based oxides, in which electrochemical cycling induces phase and compositional heterogeneity. Specifically, crystalline anatase TiO_2 undergoes a multistep transformation: initially becoming amorphous, then forming partially crystalline rock-salt $NaTiO_2$ nanograins. This transformation yields box-like cyclic voltammetry curves (Fig. 5e), characteristic of a solid-solution reaction, and results in high capacity, fast rate capability and better cycling stability[45]. Additionally, ^{7}Li solid-state NMR studies reveal reversible Li-ion shuttling between Li-poor ($Li_{0.01}TiO_2$) and Li-rich ($Li_{0.6}TiO_2$) domains within anatase TiO_2 (ref. 206) (Fig. 5f). These coexisting regions form sub-micrometre-scale phase-separated domains that are thermodynamically stable, contributing to robust and sustained electrochemical behaviour[207]. Interestingly, this spontaneous phase separation is predominantly observed in micrometre-sized particles but largely suppressed in nanoscale TiO_2, emphasizing

the size-dependent nature of phase heterogeneity[208]. Such electrochemically driven structural evolutions provide new strategies for intercalation-type electrodes with improved energy density, kinetics and long-term stability.

Modulating phase transitions. In addition to Mn-based, Nb-based and Ti-based oxides, V-based oxides also exhibit multi-electron redox chemistry and a strong tendency towards forming metastable phases during lithiation. Owing to the multiple accessible oxidation states, Li-ion insertion induces progressive atomic rearrangement to minimize free energy, often resulting in the formation of rock-salt-type structures. For instance, α-V_2O_5, composed of edge-sharing pyramidal units, undergoes a complex multi-phase evolution upon lithiation, forming a series of intermediates of $Li_xV_2O_5$ (refs. 209,210). This transformation is captured by the structural and compositional evolution in the voltage profile (Fig. 5g). Upon discharging to 1.5 V, the final product ω-$Li_3V_2O_5$ adopts a rock-salt structure, indicating substantial cation rearrangement and oxygen sublattice preservation[211]. Importantly, this framework remains structurally robust during the further delithiation, exhibiting improved structural reversibility, a highly desirable trait for long-term cycling stability.

Although disordered rock-salt oxides have been extensively explored as cathodes, their use as anodes, via deeper lithiation of already lithiated frameworks, is less studied[211–213]. In rock salt-$Li_3V_2O_5$, the oxygen ions occupy the 4*a* sites, whereas Li and V cations share the 4*b* octahedral sites with occupancies of ~52% and ~40%, respectively. A small fraction (~4%) of Li ions reside in the 8*c* tetrahedral sites. Therefore, the general formula can be expressed as $[\square_{9.6}Li_{0.4}]^{8c}[\square_{0.4}Li_{2.6}V_2]^{4b}[O_5]^{4a}$ ($\square$ = vacant site), indicating a substantial number of vacant interstitial tetrahedral sites that can host additional Li ions. Full lithiation leads to the formation of rock salt-$Li_5V_2O_5$ (ref. 122), delivering high specific capacity, fast Li-ion kinetics and a safe operating voltage.

These examples demonstrate that electrochemically induced heterogeneity, especially via controlled phase transitions towards spinel-type or rock-salt-type configurations, serves as a possible design principle for discovering metastable, high-performance electrode materials. By carefully tuning the overpotential during cycling, specific transformation pathways can be selectively activated. The optimization and design of such systems can be guided by a few critical criteria: the redox potentials and valence flexibility of TMs; the crystallographic adaptability of the parent framework; and particle size, which governs phase propagation and kinetic accessibility.

Future challenges and outlook

Despite the advantages of chemical heterogeneity, its practical implementation is not without challenges. Here, we outline key aspects, including design, synthesis, characterization and the associated challenges, that require coordinated progress to enable the continued advancement of battery technologies.

Design of chemical heterogeneity

A formidable challenge lies in the design of heterogeneity based on current scientific knowledge. This typically involves engineering intermediate or metastable states through the spatial modulation of chemical compositions, crystal structures and electrochemical reactivities, aiming to promote synergistic interactions between multiple structural motifs or functional domains. Such efforts necessitate a multidimensional design framework that integrates compositional and structural parameters. Conventional descriptors, such as ionic radius, electronegativity and elemental distribution, offer a useful starting point. However, in more complex systems, additional parameters including charge density, bonding asymmetry and local coordination environments require further exploration, as they strongly influence material behaviour and performance. In this context, ionic potentials have emerged as informative parameters, quantitatively capturing cation–anion interactions and enabling improved predictions of crystal structures and redox reversibilities[14,214–216]. To advance towards predictive design, the integration of computational tools is essential. High-throughput screening, first-principles calculations and materials informatics can accelerate the discovery of possible heterostructure materials by identifying optimal compositional and structural configurations. These approaches enable descriptor-driven design strategies, offering a potential route to tailor chemical heterogeneity for enhanced electrochemical performance.

Synthesis of chemical heterogeneity

The controlled synthesis of chemical heterogeneity is a cornerstone in the rational development of advanced battery materials. Tailoring such heterogeneity requires a careful balance between thermodynamic and kinetic accessibility. Conventional synthesis methods, such as solid-state reactions, co-precipitation and sol–gel processes, offer scalability and control of composition and phase formations[35,217]. However, generating targeted heterogeneity often requires precise tuning of various parameters such as temperature, atmosphere[218] and precursor chemistry[16]. Given that many battery materials operate far from thermodynamic equilibrium, kinetic factors play an equally important role. Electrochemical cycling, typically regarded as a performance-testing tool, has emerged as an unconventional yet effective synthesis strategy. When conducted under carefully selected conditions (such as current densities, voltage windows, depth of charge and discharge), cycling can induce metastable phase formations, trigger beneficial structural transformations and activate latent redox activities[44,45,195]. Beyond these established parameters, other less conventional factors are gaining attention for tailoring chemical heterogeneity. These include precursor reactivity, local compositional gradients, solvent effects and multistep thermal treatments that ensure the formation of different structures. Future progress will likely come from integrating thermodynamic and kinetic design principles, combined with real-time monitoring of structural evolution, to create precisely engineered heterostructures that optimize both performance and scalability.

Characterization of chemical heterogeneity

Following the successful synthesis of chemically heterogeneous structures, it becomes critically important to validate their presence and uncover the functional roles in regulating electrochemical behaviour. A comprehensive understanding requires advanced, multi-scale characterization strategies capable of capturing both static and dynamic features across different length scales[219]. At the atomic and nanoscale, heterogeneities such as lattice distortions and cation non-stoichiometry[14,40] necessitate sub-ångström resolution techniques, including advanced electron microscopy and atom probe techniques[14,40]. At the microscale, features such as phase segregation and interfacial inhomogeneity are best captured by tools like synchrotron-based X-ray diffraction, pair distribution function analysis and solid-state NMR[220–222]. Moreover, the nature of kinetic heterogeneity, especially that arising during electrochemical cycling, calls for advanced in situ and operando characterization techniques. For instance, temporally and spatially resolved synchrotron X-ray imaging

has been used to monitor phenomena such as element segregation and aggregation during battery operation[223], revealing the spatiotemporal evolution of heterostructures. These efforts underscore the urgent need for real-time, high-resolution characterization platforms capable of capturing transient, non-equilibrium states. Coupling these techniques with artificial intelligence algorithms and data-driven analytics holds great promise for unravelling complex dynamic behaviour, offering perspectives into the formation and evolution mechanisms of chemical heterogeneity across multiple length scales.

Taking advantage of chemical heterogeneity

Although chemical heterogeneity has emerged as a powerful strategy for tailoring material structures and enhancing electrochemical performance, its uncontrolled or excessive incorporation can produce detrimental effects that outweigh its benefits. At the atomic scale, overaccumulation of heteroatomic domains may disrupt local crystallographic environments, inducing lattice distortion, non-ideal bonding configurations and even partial loss of structural coherence. Such changes impede ion insertion and extraction kinetics and accelerate structural degradation, ultimately compromising specific capacity and long-term cycling stability[82,224]. These challenges are particularly evident in layered cathode materials. In Ni-rich layered oxides, excessive cation intermixing generates strong interlayer electrostatic repulsion and localized lattice strain, accelerating structural instability and capacity fading during extended cycling[93]. Similarly, Li-rich Mn-based layered cathodes suffer from TM migration and oxygen release under high-voltage operation, triggering voltage decay and phase transitions towards spinel-like or rock-salt-like structures. Surface reconstruction from layered to spinel/rock-salt phases further increases impedance and deteriorates energy efficiency[160,225,226].

Unintended compositional heterogeneity also develops during battery operation. Layered cathode particles frequently exhibit Li^+/Na^+ concentration gradients and non-uniform TM oxidation states (for example, Ni^{3+}/Ni^{4+} coexistence), generating localized high-valence domains with strong oxidizing character[227]. These domains promote lattice-oxygen release and TM-ion migration[13], reinforcing structural inhomogeneity. In $LiCoO_2$, rate-dependent state-of-charge heterogeneity can produce incompletely lithiated, electrochemically inactive regions that progressively redistribute upon cycling and are often coupled with particle cracking, establishing a direct link between chemical inhomogeneity and capacity loss[228]. For cathodes involving dominant oxygen redox processes, such as Li-rich layered oxides, oxygen-related heterogeneity becomes even more critical[229,230]. Oxygen vacancies are commonly generated when lattice oxygen participates in high-voltage redox reactions. Although moderate oxygen-vacancy formation can reduce oxygen binding energy, facilitate coupled charge transport and relieve local strain, excessive vacancy accumulation disrupts local coordination environments and induces structural collapse[231,232]. Over repeated cycling, oxygen vacancies may evolve into nanopores that initially buffer stress but subsequently act as structural weak points, accelerating voltage decay and capacity fading[233].

At larger length scales, heterogeneity-driven phase transitions and lattice volume variations during (de)lithiation generate stress concentrations at phase boundaries, leading to microcrack formation and even particle pulverization. Such effects are especially pronounced in oxide cathodes[234] and alloy-type electrodes (for example, Si-based and Sn-based systems) that undergo substantial volume expansion[235]. In solid electrolytes, poorly controlled heterogeneity can result in electrochemically inactive secondary phases that disrupt Li-ion transport continuity. For example, in garnet-type electrolytes such as $Li_7La_3Zr_2O_{12}$, unintended formation of Li-aluminate or Li-gallate phases (such as γ-$LiAlO_2$ or $LiGaO_2$) increases grain-boundary resistance and hinders interfacial ion transfer[236]. Likewise, in sulfide electrolytes such as $Li_{10}GeP_2S_{12}$, residual by-products (such as P_2S_5 or $Li_4P_2S_6$) impede long-range ion migration and destabilize electrode–electrolyte interfaces[237,238]. These examples illustrate that although deliberate chemical heterogeneity can be a design approach, unintended or parasitic heterogeneity inevitably emerges during synthesis and electrochemical operation. Such multiscale structural and compositional imbalances are closely associated with voltage decay, impedance growth and capacity fading in practical battery systems. Therefore, precise control over the composition, spatial distribution and length scale of heterogeneity is essential to harness its advantages while avoiding electrochemical penalties.

Additionally, redox heterogeneity, also a subset of chemical heterogeneity, arises from spatially non-uniform and asynchronous redox reactions within electrode materials, influencing electrochemical kinetics, structural evolution and mechanical stability. In layered oxide cathodes, such as $LiNi_{1-x-y}Mn_xCo_yO_2$ and Li-rich layered oxides, redox reactions often initiate at particle surfaces and progressively propagate towards the bulk during cycling. This spatially uneven evolution of TM oxidation states leads to compositional gradients, TM migration and surface-depletion phenomena[228,239]. In Li-rich compositions such as $Li_{1.2}Mn_{0.525}Ni_{0.175}Co_{0.1}O_2$, such redox heterogeneity is frequently accompanied by layered-to-spinel phase transitions and oxygen loss under high-voltage operation. As these transformations proceed, cathode particles may evolve from dense spherical morphologies into hollow or structurally complex architectures, reflecting the coupling of redox imbalance, lattice stress and chemo-mechanical reconstruction[225]. Surface-initiated redox heterogeneity therefore plays a dominant role in the high-voltage degradation of oxide cathodes. During electrochemical cycling, non-uniform reaction fronts and kinetic disparities within individual particles introduce localized stress concentrations and additional reactive sites, accelerating chemo-mechanical degradation. Beyond the single-particle level, statistical variations in composition, local conductivity and structural integrity among cathode particles can give rise to asynchronous electrochemical activation. Some particles become electrochemically overactivated earlier than others, experiencing amplified mechanical strain and more severe structural damage[240]. At larger length scales, repeated volumetric expansion and contraction of active materials during cycling can pulverize secondary particles or cause their detachment from the carbon–binder matrix, progressively degrading electrode integrity[241]. As rechargeable batteries advance towards thicker electrodes with reduced carbon or binder content to maximize energy density, redox heterogeneity spanning intra-particle, inter-particle, electrode and even device scales become increasingly consequential[242]. Managing such multiscale heterogeneity is therefore critical for maintaining mechanical robustness and electrochemical stability in practical high-energy-density battery systems.

Chemical heterogeneity for more systems

Beyond monovalent-ion systems, multivalent batteries, such as Mg^{2+}, Zn^{2+}, Ca^{2+} and Al^{3+}, have attracted substantial attention owing to their high volumetric capacities and intrinsic safety. However, the stronger electrostatic interactions and sluggish diffusion kinetics of multivalent ions introduce more pronounced chemical and structural heterogeneities

than those observed in monovalent systems. The high charge density of multivalent ions leads to strong Coulombic attraction with lattice anions and high de-solvation barriers, often resulting in localized intercalation pathways, spatially non-uniform site occupancy and anisotropic strain accumulation. For example, the intercalation of solvated Mg ions into layered semi-conductive MoS_2 induces metastable domains with heterogeneous coordination environments[243]. Notably, the metallic MoS_2 structure facilitates rapid electron transfer, partially compensating for the large Mg^{2+} diffusion barrier. Similarly, heterogeneous oxides can reversibly accommodate Ca-ion insertion by integrating multiple sub-phases with distinct oxygen coordination environments, thereby alleviating the strain associated with multivalent insertion[244]. Beyond intercalation chemistries, multivalent systems frequently undergo conversion-type reactions, which inherently generate phase and redox heterogeneity at multiple length scales. In such cases, dynamic coexistence of intermediate phases and local charge redistribution can act as adaptive buffers, mitigating strong ion–lattice coupling and suppressing catastrophic structural collapse. Chemical heterogeneity in multivalent systems should not be regarded merely as a by-product of strong ion–lattice interactions, but rather as a tuneable structural motif that can regulate charge distribution, relieve mechanical stress and mediate sluggish reaction kinetics.

Conclusions

In this Review, we discuss the concept of chemical heterogeneity across multiple length scales, emphasizing its role in developing high-performance electrodes and electrolytes. At the atomic scale and nanoscale, local compositional fluctuations and nano-domains disrupt long-range order, modulate ion transport and stabilize redox activity. At larger scales towards the microscale, purposefully engineered multiphase architectures, through phase intergrowth, can simultaneously enhance energy density, mechanical robustness and interfacial stability. Beyond thermodynamical equilibrium considerations, kinetically driven processes during electrochemical cycling can generate metastable heterostructures with improved functionalities, such as improved rate capability and structural resilience, thereby broadening the design space for advanced battery materials. Overall, the chemical heterogeneity represents a promising yet underexplored strategy for optimizing the structure–function relationships of battery materials.

Realizing its full potential will require coordinated advancements across multiple disciplines, including synthesis methodologies, multi-scale characterization techniques, theoretical modelling and data-driven materials design. In particular, achieving precise and predictive control of chemical heterogeneity is critical for the rational development of next-generation battery materials, as it allows researchers to systematically tailor local chemical environments and fine-tune electrochemical performance, structural stability and interfacial behaviour. Although this Review primarily focuses on heterogeneity at the single-particle level, chemical heterogeneities at the inter-particle, electrode and device levels also play decisive roles in governing electron and ion transport and, ultimately, overall electrochemical performance. A deeper mechanistic understanding of these multiscale heterogeneities, whether beneficial or detrimental, will be crucial for guiding rational materials design and lifetime optimization. By transforming chemical heterogeneity from an empirical observation into a predictive design principle, the field can not only accelerate progress in energy storage technologies but also inspire the broader development of multifunctional materials across diverse applications.

Published online: 21 April 2026

References

1. Armand, M. & Tarascon, J.-M. Building better batteries. *Nature* **451**, 652–657 (2008).
2. Dunn, B., Kamath, H. & Tarascon, J.-M. Electrical energy storage for the grid: a battery of choices. *Science* **334**, 928–935 (2011).
3. Goodenough, J. B. & Park, K.-S. The Li-ion rechargeable battery: a perspective. *J. Am. Chem. Soc.* **135**, 1167–1176 (2013).
4. Liu, Z., Yu, A. & Lee, J. Y. Synthesis and characterization of $LiNi_{1-x-y}Co_xMn_yO_2$ as the cathode materials of secondary lithium batteries. *J. Power Sources* **81-82**, 416–419 (1999).
5. Padhi, A. K., Nanjundaswamy, K. S. & Goodenough, J. B. Phospho-olivines as positive-electrode materials for rechargeable lithium batteries. *J. Electrochem. Soc.* **144**, 1188 (1997).
6. Whittingham, M. S. Electrical energy storage and intercalation chemistry. *Science* **192**, 1126–1127 (1976).
7. Mizushima, K., Jones, P. C., Wiseman, P. J. & Goodenough, J. B. Li_xCoO_2 (0<x<–1): a new cathode material for batteries of high energy density. *Mater. Res. Bull.* **15**, 783–789 (1980).
8. Ozawa, K. Lithium-ion rechargeable batteries with $LiCoO_2$ and carbon electrodes: the $LiCoO_2$/C system. *Solid State Ion.* **69**, 212–221 (1994).
9. Zhong, Q., Bonakdarpour, A., Zhang, M., Gao, Y. & Dahn, J. R. Synthesis and electrochemistry of $LiNi_xMn_{2-x}O_4$. *J. Electrochem. Soc.* **144**, 205 (1997).
10. Thackeray, M. M., David, W. I. F., Bruce, P. G. & Goodenough, J. B. Lithium insertion into manganese spinels. *Mater. Res. Bull.* **18**, 461–472 (1983).
11. Friedrich, F. et al. Editors' choice—capacity fading mechanisms of NCM-811 cathodes in lithium-ion batteries studied by X-ray diffraction and other diagnostics. *J. Electrochem. Soc.* **166**, A3760 (2019).
12. Ryu, H.-H., Park, K.-J., Yoon, C. S. & Sun, Y.-K. Capacity fading of Ni-rich $Li[Ni_xCo_yMn_{1-x-y}]O_2$ ($0.6\leq x\leq 0.95$) cathodes for high-energy-density lithium-ion batteries: bulk or surface degradation? *Chem. Mater.* **30**, 1155–1163 (2018).
13. Xu, C. et al. Bulk fatigue induced by surface reconstruction in layered Ni-rich cathodes for Li-ion batteries. *Nat. Mater.* **20**, 84–92 (2021).
14. Wang, Q. et al. Chemical short-range disorder in lithium oxide cathodes. *Nature* **629**, 341–347 (2024).
15. Xu, H. et al. Guiding the design of heterogeneous electrode microstructures for Li-ion batteries: microscopic imaging, predictive modeling, and machine learning. *Adv. Energy Mater.* **11**, 2003908 (2021).
16. Zhang, J.-N. et al. Trace doping of multiple elements enables stable battery cycling of $LiCoO_2$ at 4.6 V. *Nat. Energy* **4**, 594–603 (2019).
17. Xu, Z. et al. Charge distribution guided by grain crystallographic orientations in polycrystalline battery materials. *Nat. Commun.* **11**, 83 (2020).
18. Kang, S., Lee, S., Lee, H. & Kang, Y.-M. Manipulating disorder within cathodes of alkali-ion batteries. *Nat. Rev. Chem.* **8**, 587–604 (2024).
19. Zhu, Y. & Wu, X. Heterostructured materials. *Prog. Mater. Sci.* **131**, 101019 (2023).
20. Wu, X. & Zhu, Y. Heterogeneous materials: a new class of materials with unprecedented mechanical properties. *Mater. Res. Lett.* **5**, 527–532 (2017).
21. Ashby, M. F. The deformation of plastically non-homogeneous materials. *Philos. Mag.* **21**, 399–424 (1970).
22. Bender, T. A., Dabrowski, J. A. & Gagné, M. R. Homogeneous catalysis for the production of low-volume, high-value chemicals from biomass. *Nat. Rev. Chem.* **2**, 35–46 (2018).
23. Copéret, C., Chabanas, M., Petroff Saint-Arroman, R. & Basset, J.-M. Homogeneous and heterogeneous catalysis: bridging the gap through surface organometallic chemistry. *Angew. Chem. Int. Ed.* **42**, 156–181 (2003).
24. Yao, Z. et al. Homogeneous/inhomogeneous-structured dielectrics and their energy-storage performances. *Adv. Mater.* **29**, 1601727 (2017).
25. Wang, Y., Waterhouse, G. I. N., Shang, L. & Zhang, T. Electrocatalytic oxygen reduction to hydrogen peroxide: from homogeneous to heterogeneous electrocatalysis. *Adv. Energy Mater.* **11**, 2003323 (2021).
26. McDowell, D. L. Viscoplasticity of heterogeneous metallic materials. *Mater. Sci. Eng. R Rep.* **62**, 67–123 (2008).
27. Ma, E. & Zhu, T. Towards strength–ductility synergy through the design of heterogeneous nanostructures in metals. *Mater. Today* **20**, 323–331 (2017).
28. Sathiyamoorthi, P. & Kim, H. S. High-entropy alloys with heterogeneous microstructure: processing and mechanical properties. *Prog. Mater. Sci.* **123**, 100709 (2022).
29. Yang, Y. et al. Quantification of heterogeneous degradation in Li-ion batteries. *Adv. Energy Mater.* **9**, 1900674 (2019).
30. Pandya, R. et al. Three-dimensional operando optical imaging of particle and electrolyte heterogeneities inside Li-ion batteries. *Nat. Nanotechnol.* **18**, 1185–1194 (2023).
31. Liu, H. et al. Capturing metastable structures during high-rate cycling of $LiFePO_4$ nanoparticle electrodes. *Science* **344**, 1252817 (2014).
32. Suresh, S. Graded materials for resistance to contact deformation and damage. *Science* **292**, 2447–2451 (2001).
33. Hyooma, H. & Hayashi, K. Crystal structures of $La_3Li_5M_2O_{12}$ (M=Nb, Ta). *Mater. Res. Bull.* **23**, 1399–1407 (1988).
34. Murugan, R., Thangadurai, V. & Weppner, W. Fast lithium ion conduction in garnet-type $Li_7La_3Zr_2O_{12}$. *Angew. Chem. Int. Ed.* **46**, 7778–7781 (2007).
35. Rossen, E., Reimers, J. N. & Dahn, J. R. Synthesis and electrochemistry of spinel LT $LiCoO_2$. *Solid State Ion.* **62**, 53–60 (1993).
36. Maiyalagan, T., Jarvis, K. A., Therese, S., Ferreira, P. J. & Manthiram, A. Spinel-type lithium cobalt oxide as a bifunctional electrocatalyst for the oxygen evolution and oxygen reduction reactions. *Nat. Commun.* **5**, 3949 (2014).

37. Maier, J. Review—battery materials: why defect chemistry? *J. Electrochem. Soc.* **162**, A2380 (2015).
38. Wu, H. & Fan, G. An overview of tailoring strain delocalization for strength-ductility synergy. *Prog. Mater. Sci.* **113**, 100675 (2020).
39. Azizi, H. et al. Using architectured materials to control localized shear fracture. *Acta Mater.* **143**, 298–305 (2018).
40. Yang, T. et al. Ultrahigh-nickel layered cathode with cycling stability for sustainable lithium-ion batteries. *Nat. Sustain.* **7**, 1204–1214 (2024).
41. Li, L. et al. Atomic-scale probing of short-range order and its impact on electrochemical properties in cation-disordered oxide cathodes. *Nat. Commun.* **14**, 7448 (2023).
42. Yang, Y. et al. Expandable fast Li-ion diffusion network of Li-rich Mn-based oxides via single-layer $LiCo(Ni)O_2$ segregation. *Adv. Mater.* **37**, 2414786 (2025).
43. Li, B. et al. Constructing "Li-rich Ni-rich" oxide cathodes for high-energy-density Li-ion batteries. *Energy Environ. Sci.* **16**, 1210–1222 (2023).
44. Barnes, P. et al. Electrochemically induced amorphous-to-rock-salt phase transformation in niobium oxide electrode for Li-ion batteries. *Nat. Mater.* **21**, 795–803 (2022).
45. Tang, D. et al. Electrochemically in situ formed rocksalt phase in titanium dioxide determines pseudocapacitive sodium-ion storage. *Nat. Commun.* **16**, 2015 (2025).
46. Li, L. et al. Fluorination-enhanced surface stability of cation-disordered rocksalt cathodes for Li-Ion batteries. *Adv. Funct. Mater.* **31**, 2101888 (2021).
47. Zhu, X., Cao, G., Liu, J., Zhao, K. & An, L. Enhanced strength and ductility synergy in aluminum composite with heterogeneous structure. *Mater. Sci. Eng. A* **787**, 139431 (2020).
48. Zhu, Y. Introduction to heterostructured materials: a fast emerging field. *Metall. Mater. Trans. A* **52**, 4715–4726 (2021).
49. Dong, X. et al. Heterostructured metallic structural materials: research methods, properties, and future perspectives. *Adv. Funct. Mater.* **34**, 2410521 (2024).
50. Lu, K. Making strong nanomaterials ductile with gradients. *Science* **345**, 1455–1456 (2014).
51. Fang, T. H., Li, W. L., Tao, N. R. & Lu, K. Revealing extraordinary intrinsic tensile plasticity in gradient nano-grained copper. *Science* **331**, 1587–1590 (2011).
52. Zhu, Y. T. & Liao, X. Retaining ductility. *Nat. Mater.* **3**, 351–352 (2004).
53. Wu, X. et al. Nanodomained nickel unite nanocrystal strength with coarse-grain ductility. *Sci. Rep.* **5**, 11728 (2015).
54. Lu, K., Yan, F. K., Wang, H. T. & Tao, N. R. Strengthening austenitic steels by using nanotwinned austenitic grains. *Scr. Mater.* **66**, 878–883 (2012).
55. Frohna, K. et al. Nanoscale chemical heterogeneity dominates the optoelectronic response of alloyed perovskite solar cells. *Nat. Nanotechnol.* **17**, 190–196 (2022).
56. Correa-Baena, J.-P. et al. Homogenized halides and alkali cation segregation in alloyed organic-inorganic perovskites. *Science* **363**, 627–631 (2019).
57. Feldmann, S. et al. Photodoping through local charge carrier accumulation in alloyed hybrid perovskites for highly efficient luminescence. *Nat. Photonics* **14**, 123–128 (2020).
58. Zhao, L.-D. et al. Ultralow thermal conductivity and high thermoelectric figure of merit in SnSe crystals. *Nature* **508**, 373–377 (2014).
59. Jiang, Y. et al. Heterogeneous silicon mesostructures for lipid-supported bioelectric interfaces. *Nat. Mater.* **15**, 1023–1030 (2016).
60. Yi, J. et al. Water-responsive supercontractile polymer films for bioelectronic interfaces. *Nature* **624**, 295–302 (2023).
61. Delmas, C., Fouassier, C. & Hagenmuller, P. Structural classification and properties of the layered oxides. *Physica B+C* **99**, 81–85 (1980).
62. Reimers, J. N. & Dahn, J. R. Electrochemical and in situ X-ray diffraction studies of lithium intercalation in Li_xCoO_2. *J. Electrochem. Soc.* **139**, 2091–2097 (1992).
63. Shao-Horn, Y., Levasseur, S., Weill, F. & Delmas, C. Probing lithium and vacancy ordering in O3 layered Li_xCoO_2 (x≈0.5). *J. Electrochem. Soc.* **150**, A366 (2003).
64. Chen, Z., Lu, Z. & Dahn, J. R. Staging phase transitions in Li_xCoO_2. *J. Electrochem. Soc.* **149**, A1604 (2002).
65. Van der Ven, A., Aydinol, M. K., Ceder, G., Kresse, G. & Hafner, J. First-principles investigation of phase stability in Li_xCoO_2. *Phys. Rev. B* **58**, 2975–2987 (1998).
66. Amatucci, G. G., Tarascon, J. M. & Klein, L. C. CoO_2, the end member of the Li_xCoO_2 solid solution. *J. Electrochem. Soc.* **143**, 1114–1123 (1996).
67. Yang, Y. et al. Determining the three-dimensional atomic structure of an amorphous solid. *Nature* **592**, 60–64 (2021).
68. Sheng, H. W., Luo, W. K., Alamgir, F. M., Bai, J. M. & Ma, E. Atomic packing and short-to-medium-range order in metallic glasses. *Nature* **439**, 419–425 (2006).
69. Yeh, J. W. et al. Nanostructured high-entropy alloys with multiple principal elements: novel alloy design concepts and outcomes. *Adv. Eng. Mater.* **6**, 299–303 (2004).
70. Cantor, B., Chang, I. T. H., Knight, P. & Vincent, A. J. B. Microstructural development in equiatomic multicomponent alloys. *Mater. Sci. Eng. A* **375-377**, 213–218 (2004).
71. Yang, T. et al. Multicomponent intermetallic nanoparticles and superb mechanical behaviors of complex alloys. *Science* **362**, 933–937 (2018).
72. Zhang, R. et al. Short-range order and its impact on the CrCoNi medium-entropy alloy. *Nature* **581**, 283–287 (2020).
73. Ding, J., Yu, Q., Asta, M. & Ritchie, R. O. Tunable stacking fault energies by tailoring local chemical order in CrCoNi medium-entropy alloys. *Proc. Natl Acad. Sci. USA* **115**, 8919–8924 (2018).
74. Dahn, J. R., von Sacken, U., Juzkow, M. W. & Al-Janaby, H. Rechargeable $LiNiO_2$/carbon cells. *J. Electrochem. Soc.* **138**, 2207 (1991).
75. Yamada, S., Fujiwara, M. & Kanda, M. Synthesis and properties of $LiNiO_2$ as cathode material for secondary batteries. *J. Power Sources* **54**, 209–213 (1995).
76. Bianchini, M., Roca-Ayats, M., Hartmann, P., Brezesinski, T. & Janek, J. There and back again—the journey of $LiNiO_2$ as a cathode active material. *Angew. Chem. Int. Ed.* **58**, 10434–10458 (2019).
77. Park, G.-T. et al. Introducing high-valence elements into cobalt-free layered cathodes for practical lithium-ion batteries. *Nat. Energy* **7**, 946–954 (2022).
78. Yu, H. et al. Surface enrichment and diffusion enabling gradient-doping and coating of Ni-rich cathode toward Li-ion batteries. *Nat. Commun.* **12**, 4564 (2021).
79. Jung, R., Metzger, M., Maglia, F., Stinner, C. & Gasteiger, H. A. Oxygen release and its effect on the cycling stability of $LiNi_xMn_yCo_zO_2$ (NMC) cathode materials for Li-ion batteries. *J. Electrochem. Soc.* **164**, A1361 (2017).
80. Lee, S.-W. et al. Li_3PO_4 surface coating on Ni-rich $LiNi_{0.6}Co_{0.2}Mn_{0.2}O_2$ by a citric acid assisted sol-gel method: improved thermal stability and high-voltage performance. *J. Power Sources* **360**, 206–214 (2017).
81. Kim, U. H. et al. Pushing the limit of layered transition metal oxide cathodes for high-energy density rechargeable Li ion batteries. *Energy Environ. Sci.* **11**, 1271–1279 (2018).
82. Sun, H. H. et al. Transition metal-doped Ni-rich layered cathode materials for durable Li-ion batteries. *Nat. Commun.* **12**, 6552 (2021).
83. Kim, U.-H. et al. Heuristic solution for achieving long-term cycle stability for Ni-rich layered cathodes at full depth of discharge. *Nat. Energy* **5**, 860–869 (2020).
84. Kong, D. et al. Ti-gradient doping to stabilize layered surface structure for high performance high-Ni oxide cathode of Li-ion battery. *Adv. Energy Mater.* **9**, 1901756 (2019).
85. Park, G.-T., Ryu, H.-H., Noh, T.-C., Kang, G.-C. & Sun, Y.-K. Microstructure-optimized concentration-gradient NCM cathode for long-life Li-ion batteries. *Mater. Today* **52**, 9–18 (2022).
86. Sathiya, M. et al. Li_4NiTeO_6 as a positive electrode for Li-ion batteries. *Chem. Commun.* **49**, 11376–11378 (2013).
87. Lee, J. et al. Unlocking the potential of cation-disordered oxides for rechargeable lithium batteries. *Science* **343**, 519–522 (2014).
88. Lun, Z. et al. Cation-disordered rocksalt-type high-entropy cathodes for Li-ion batteries. *Nat. Mater.* **20**, 214–221 (2021).
89. Clément, R. J., Kitchaev, D., Lee, J. & Gerbrand, C. Short-range order and unusual modes of nickel redox in a fluorine-substituted disordered rocksalt oxide lithium-ion cathode. *Chem. Mater.* **30**, 6945–6956 (2018).
90. Seo, D.-H. et al. The structural and chemical origin of the oxygen redox activity in layered and cation-disordered Li-excess cathode materials. *Nat. Chem.* **8**, 692–697 (2016).
91. Ji, H. et al. Hidden structural and chemical order controls lithium transport in cation-disordered oxides for rechargeable batteries. *Nat. Commun.* **10**, 592 (2019).
92. Wang, Q. et al. Designing lithium halide solid electrolytes. *Nat. Commun.* **15**, 1050 (2024).
93. Deng, Y. et al. Crystal structures, local atomic environments, and ion diffusion mechanisms of scandium-substituted sodium superionic conductor (NASICON) solid electrolytes. *Chem. Mater.* **30**, 2618–2630 (2018).
94. Janek, J. & Zeier, W. G. A solid future for battery development. *Nat. Energy* **1**, 16141 (2016).
95. Jun, K., Chen, Y., Wei, G., Yang, X. & Ceder, G. Diffusion mechanisms of fast lithium-ion conductors. *Nat. Rev. Mater.* **9**, 887–905 (2024).
96. Liang, Z., Du, F., Zhao, N. & Guo, X. Revealing the reason for the unsuccessful fabrication of $Li_3Zr_2Si_2PO_{12}$ by solid state reaction. *Chin. J. Struct. Chem.* **42**, 100108 (2023).
97. Di Stefano, D. et al. Superionic diffusion through frustrated energy landscape. *Chem* **5**, 2450–2460 (2019).
98. Jalem, R. et al. Effects of gallium doping in garnet-type $Li_7La_3Zr_2O_{12}$ solid electrolytes. *Chem. Mater.* **27**, 2821–2831 (2015).
99. Posch, P. et al. Ion dynamics in Al-stabilized $Li_7La_3Zr_2O_{12}$ single crystals—macroscopic transport and the elementary steps of ion hopping. *Energy Storage Mater.* **24**, 220–228 (2020).
100. Gao, S. et al. Hydride-based antiperovskites with soft anionic sublattices as fast alkali ionic conductors. *Nat. Commun.* **12**, 201 (2021).
101. Wang, Y. et al. Antiperovskites with exceptional functionalities. *Adv. Mater.* **32**, 1905007 (2020).
102. Hood, Z. D., Wang, H., Samuthira Pandian, A., Keum, J. K. & Liang, C. Li_2OHCl crystalline electrolyte for stable metallic lithium anodes. *J. Am. Chem. Soc.* **138**, 1768–1771 (2016).
103. Wang, F. et al. Dynamics of hydroxyl anions promotes lithium ion conduction in antiperovskite Li_2OHCl. *Chem. Mater.* **32**, 8481–8491 (2020).
104. Gao, L. et al. Boosting lithium ion conductivity of antiperovskite solid electrolyte by potassium ions substitution for cation clusters. *Nat. Commun.* **14**, 6807 (2023).
105. Li, H. et al. Toward high-energy Mn-based disordered-rocksalt Li-ion cathodes. *Joule* **6**, 53–91 (2022).
106. Freire, M. et al. A new active Li–Mn–O compound for high energy density Li-ion batteries. *Nat. Mater.* **15**, 173–177 (2016).
107. Liu, T. et al. Origin of structural degradation in Li-rich layered oxide cathode. *Nature* **606**, 305–312 (2022).
108. Takeda, N. et al. Reversible Li storage for nanosize cation/anion-disordered rocksalt-type oxyfluorides: $LiMoO_2$-$xLiF$ ($0 \le x \le 2$) binary system. *J. Power Sources* **367**, 122–129 (2017).
109. Lee, J. et al. Reversible Mn^{2+}/Mn^{4+} double redox in lithium-excess cathode materials. *Nature* **556**, 185–190 (2018).
110. Cai, Z. et al. In situ formed partially disordered phases as earth-abundant Mn-rich cathode materials. *Nat. Energy* **9**, 27–36 (2024).

111. Li, L. et al. Fluorination-enhanced surface stability of disordered rocksalt cathodes. *Adv. Mater.* **34**, 2106256 (2022).
112. Tsuzuki, T. Mechanochemical synthesis of metal oxide nanoparticles. *Commun. Chem.* **4**, 143 (2021).
113. Clément, R. J., Lun, Z. & Ceder, G. Cation-disordered rocksalt transition metal oxides and oxyfluorides for high energy lithium-ion cathodes. *Energy Environ. Sci.* **13**, 345–373 (2020).
114. Zhang, Y. et al. Investigating particle size-dependent redox kinetics and charge distribution in disordered rocksalt cathodes. *Adv. Funct. Mater.* **32**, 2110502 (2022).
115. Hau, H.-M. et al. Earth-abundant Li-ion cathode materials with nanoengineered microstructures. *Nat. Nanotechnol.* **19**, 1831–1839 (2024).
116. Thackeray, M. M. et al. Spinel electrodes from the Li-Mn-O system for rechargeable lithium battery applications. *J. Electrochem. Soc.* **139**, 363 (1992).
117. Barker, J., Koksbang, R. & Saïdi, M. Y. Lithium insertion in manganese oxides: a model lithium ion system. *Solid State Ion.* **82**, 143–151 (1995).
118. Chen, T., Yang, J., Barroso-Luque, L. & Ceder, G. Removing the two-phase transition in spinel $LiMn_2O_4$ through cation disorder. *ACS Energy Lett.* **8**, 314–319 (2023).
119. Ahn, J. et al. Ultrahigh-capacity rocksalt cathodes enabled by cycling-activated structural changes. *Adv. Energy Mater.* **13**, 2300221 (2023).
120. Ahn, J. et al. Exceptional cycling performance enabled by local structural rearrangements in disordered rocksalt cathodes. *Adv. Energy Mater.* **12**, 2200426 (2022).
121. Liu, Y. et al. A partially disordered crystallographic shear block structure as fast-charging negative electrode material for lithium-ion batteries. *Nat. Commun.* **16**, 6507 (2025).
122. Liu, H. et al. A disordered rock salt anode for fast-charging lithium-ion batteries. *Nature* **585**, 63–67 (2020).
123. Yabuuchi, N. et al. High-capacity electrode materials for rechargeable lithium batteries: Li_3NbO_4-based system with cation-disordered rocksalt structure. *Proc. Natl Acad. Sci. USA* **112**, 7650–7655 (2015).
124. Zhou, Y., Xu, Y., Song, J. & Tan, Q. Preparation and performance investigation of carbon-coated $Li_{1.2}Mn_{0.2}Ti_{0.6}O_2$/C cathode materials. *ACS Appl. Mater. Interfaces* **16**, 52539–52549 (2024).
125. Ahn, J., Chen, D. & Chen, G. A fluorination method for improving cation-disordered rocksalt cathode performance. *Adv. Energy Mater.* **10**, 2001671 (2020).
126. Leifer, N. et al. Linking structure to performance of $Li_{1.2}Mn_{0.54}Ni_{0.13}Co_{0.13}O_2$ (Li and Mn rich NMC) cathode materials synthesized by different methods. *Phys. Chem. Chem. Phys.* **22**, 9098–9109 (2020).
127. Zhang, M. et al. Pushing the limit of *3d* transition metal-based layered oxides that use both cation and anion redox for energy storage. *Nat. Rev. Mater.* **7**, 522–540 (2022).
128. McColl, K., Coles, S. W., Zarabadi-Poor, P., Morgan, B. J. & Islam, M. S. Phase segregation and nanoconfined fluid O_2 in a lithium-rich oxide cathode. *Nat. Mater.* **23**, 826–833 (2024).
129. Hong, J. et al. Metal–oxygen decoordination stabilizes anion redox in Li-rich oxides. *Nat. Mater.* **18**, 256–265 (2019).
130. Gent, W. E., Abate, I. I., Yang, W., Nazar, L. F. & Chueh, W. C. Design rules for high-valent redox in intercalation electrodes. *Joule* **4**, 1369–1397 (2020).
131. Gent, W. E. et al. Coupling between oxygen redox and cation migration explains unusual electrochemistry in lithium-rich layered oxides. *Nat. Commun.* **8**, 2091 (2017).
132. Li, B. et al. Correlating ligand-to-metal charge transfer with voltage hysteresis in a Li-rich rock-salt compound exhibiting anionic redox. *Nat. Chem.* **13**, 1070–1080 (2021).
133. Zhuo, H. et al. Atomic-scale revealing the structure distribution between $LiMO_2$ and Li_2MnO_3 in Li-rich and Mn-based oxide cathode materials. *Adv. Energy Mater.* **13**, 2203354 (2023).
134. Rozier, P. & Tarascon, J. M. Review—Li-rich layered oxide cathodes for next-generation Li-ion batteries: chances and challenges. *J. Electrochem. Soc.* **162**, A2490 (2015).
135. Assat, G. & Tarascon, J.-M. Fundamental understanding and practical challenges of anionic redox activity in Li-ion batteries. *Nat. Energy* **3**, 373–386 (2018).
136. Li, M. et al. Cationic and anionic redox in lithium-ion based batteries. *Chem. Soc. Rev.* **49**, 1688–1705 (2020).
137. Liu, J. et al. Anionic redox induced anomalous structural transition in Ni-rich cathodes. *Energy Environ. Sci.* **14**, 6441–6454 (2021).
138. Dixit, M., Markovsky, B., Schipper, F., Aurbach, D. & Major, D. T. Origin of structural degradation during cycling and low thermal stability of Ni-rich layered transition metal-based electrode materials. *J. Phys. Chem. C* **121**, 22628–22636 (2017).
139. Yoon, C. S., Jun, D.-W., Myung, S.-T. & Sun, Y.-K. Structural stability of $LiNiO_2$ cycled above 4.2 V. *ACS Energy Lett.* **2**, 1150–1155 (2017).
140. Li, J., Downie, L. E., Ma, L., Qiu, W. & Dahn, J. R. Study of the failure mechanisms of $LiNi_{0.8}Mn_{0.1}Co_{0.1}O_2$ cathode material for lithium ion batteries. *J. Electrochem. Soc.* **162**, A1401 (2015).
141. Lee, E.-J. et al. Development of microstrain in aged lithium transition metal oxides. *Nano Lett.* **14**, 4873–4880 (2014).
142. Jung, C.-H. et al. Revisiting the role of Zr doping in Ni-rich layered cathodes for lithium-ion batteries. *J. Mater. Chem. A* **9**, 17415–17424 (2021).
143. Kumari, P. & Kundu, R. Outlook of doping engineering in NMC and LMNO cathode materials for next-generation Li-ion batteries. *Energy Fuels* **39**, 10933–10966 (2025).
144. Gao, B., Jalem, R. & Tateyama, Y. Atomistic insight into the dopant impacts at the garnet $Li_7La_3Zr_2O_{12}$ solid electrolyte grain boundaries. *J. Mater. Chem. A* **10**, 10083–10091 (2022).
145. Zhao, Q., Stalin, S., Zhao, C.-Z. & Archer, L. A. Designing solid-state electrolytes for safe, energy-dense batteries. *Nat. Rev. Mater.* **5**, 229–252 (2020).
146. Fang, C.-D. et al. Revealing and reconstructing the 3D Li-ion transportation network for superionic poly(ethylene) oxide conductor. *Nat. Commun.* **15**, 6781 (2024).
147. Berthier, C. et al. Microscopic investigation of ionic conductivity in alkali metal salts-poly(ethylene oxide) adducts. *Solid State Ion.* **11**, 91–95 (1983).
148. Hamaide, T., Carre, C. & Guyot, A. Influence of the PEO macromonomers on the ionic transport and aging processes in heterogeneous solid polymer electrolytes: a fractal approach. *Solid State Ion.* **39**, 173–186 (1990).
149. Gadjourova, Z., Andreev, Y. G., Tunstall, D. P. & Bruce, P. G. Ionic conductivity in crystalline polymer electrolytes. *Nature* **412**, 520–523 (2001).
150. Croce, F., Appetecchi, G. B., Persi, L. & Scrosati, B. Nanocomposite polymer electrolytes for lithium batteries. *Nature* **394**, 456–458 (1998).
151. Zhang, W. et al. Single-phase local-high-concentration solid polymer electrolytes for lithium-metal batteries. *Nat. Energy* **9**, 386–400 (2024).
152. Yu, Z. et al. Dendrites in solid-state batteries: ion transport behavior, advanced characterization, and interface regulation. *Adv. Energy Mater.* **11**, 2003250 (2021).
153. Xu, S. et al. Decoupling of ion pairing and ion conduction in ultrahigh-concentration electrolytes enables wide-temperature solid-state batteries. *Energy Environ. Sci.* **15**, 3379–3387 (2022).
154. Tang, L. et al. Polyfluorinated crosslinker-based solid polymer electrolytes for long-cycling 4.5 V lithium metal batteries. *Nat. Commun.* **14**, 2301 (2023).
155. Mi, J. et al. Topology crafting of polyvinylidene difluoride electrolyte creates ultra-long cycling high-voltage lithium metal solid-state batteries. *Energy Storage Mater.* **48**, 375–383 (2022).
156. Urban, A., Lee, J. & Ceder, G. The configurational space of rocksalt-type oxides for high-capacity lithium battery electrodes. *Adv. Energy Mater.* **4**, 1400478 (2014).
157. Gummow, R. J., de Kock, A. & Thackeray, M. M. Improved capacity retention in rechargeable 4 V lithium/lithium-manganese oxide (spinel) cells. *Solid State Ion.* **69**, 59–67 (1994).
158. Bianchini, M., Suard, E., Croguennec, L. & Masquelier, C. Li-rich $Li_{1+x}Mn_{2-x}O_4$ spinel electrode materials: an operando neutron diffraction study during Li^+ extraction/insertion. *J. Phys. Chem. C* **118**, 25947–25955 (2014).
159. Cai, Z. et al. Realizing continuous cation order-to-disorder tuning in a class of high-energy spinel-type Li-ion cathodes. *Matter* **4**, 3897–3916 (2021).
160. Armstrong, A. R. et al. Demonstrating oxygen loss and associated structural reorganization in the lithium battery cathode $Li[Ni_{0.2}Li_{0.2}Mn_{0.6}]O_2$. *J. Am. Chem. Soc.* **128**, 8694–8698 (2006).
161. Luo, K. et al. Charge-compensation in *3d*-transition-metal-oxide intercalation cathodes through the generation of localized electron holes on oxygen. *Nat. Chem.* **8**, 684–691 (2016).
162. Lun, Z. et al. Improved cycling performance of Li-excess cation-disordered cathode materials upon fluorine substitution. *Adv. Energy Mater.* **9**, 1802959 (2019).
163. Kitchaev, D. A. et al. Design principles for high transition metal capacity in disordered rocksalt Li-ion cathodes. *Energy Environ. Sci.* **11**, 2159–2171 (2018).
164. Ji, H. et al. Ultrahigh power and energy density in partially ordered lithium-ion cathode materials. *Nat. Energy* **5**, 213–221 (2020).
165. Chen, Z., Du, T., Krishnan, N. M. A., Yue, Y. & Smedskjaer, M. M. Disorder-induced enhancement of lithium-ion transport in solid-state electrolytes. *Nat. Commun.* **16**, 1057 (2025).
166. Xue, P. et al. Structure-induced partial phase transformation endows hollow TiO_2/TiN heterostructure fibers stacked with nanosheet arrays with extraordinary sodium storage performance. *J. Mater. Chem. A* **9**, 12109–12118 (2021).
167. Yoon, M. et al. Reactive boride infusion stabilizes Ni-rich cathodes for lithium-ion batteries. *Nat. Energy* **6**, 362–371 (2021).
168. Xu, C., Reeves, P. J., Jacquet, Q. & Grey, C. P. Phase behavior during electrochemical cycling of Ni-rich cathode materials for Li-ion batteries. *Adv. Energy Mater.* **11**, 2003404 (2021).
169. Wang, L., Liu, T., Wu, T. & Lu, J. Strain-retardant coherent perovskite phase stabilized Ni-rich cathode. *Nature* **611**, 61–67 (2022).
170. Burley, J. C. et al. Magnetism and structural chemistry of the *n*=1 Ruddlesden–Popper phases La_4LiMnO_8 and $La_3SrLiMnO_8$. *J. Am. Chem. Soc.* **124**, 620–628 (2002).
171. Lee, E. et al. Layered P2/O3 intergrowth cathode: toward high power Na-ion batteries. *Adv. Energy Mater.* **4**, 1400458 (2014).
172. Tsukasaki, H., Mori, S., Shiotani, S. & Yamamura, H. Ionic conductivity and crystallization process in the Li_2S–P_2S_5 glass electrolyte. *Solid State Ion.* **317**, 122–126 (2018).
173. Sata, N., Eberman, K., Eberl, K. & Maier, J. Mesoscopic fast ion conduction in nanometre-scale planar heterostructures. *Nature* **408**, 946–949 (2000).
174. Yamada, H., Bhattacharyya, A. J. & Maier, J. Extremely high silver ionic conductivity in composites of silver halide (AgBr, AgI) and mesoporous alumina. *Adv. Funct. Mater.* **16**, 525–530 (2006).
175. Wang, R. et al. Twin boundary defect engineering improves lithium-ion diffusion for fast-charging spinel cathode materials. *Nat. Commun.* **12**, 3085 (2021).
176. Wang, Y. et al. Self-organized hetero-nanodomains actuating super Li^+ conduction in glass ceramics. *Nat. Commun.* **14**, 669 (2023).
177. Lin, X. et al. A family of dual-anion-based sodium superionic conductors for all-solid-state sodium-ion batteries. *Nat. Mater.* **24**, 83–91 (2025).
178. Fu, J. et al. Superionic conducting halide frameworks enabled by interface-bonded halides. *J. Am. Chem. Soc.* **145**, 2183–2194 (2023).
179. Jin, C. et al. Inhibiting and rejuvenating dead lithium in battery materials. *Nat. Rev. Chem.* **9**, 553–568 (2025).

180. Lin, D., Liu, Y. & Cui, Y. Reviving the lithium metal anode for high-energy batteries. *Nat. Nanotechnol.* **12**, 194–206 (2017).
181. Wan, J. et al. Ultrathin, flexible, solid polymer composite electrolyte enabled with aligned nanoporous host for lithium batteries. *Nat. Nanotechnol.* **14**, 705–711 (2019).
182. Zhao, Q., Liu, X., Stalin, S., Khan, K. & Archer, L. A. Solid-state polymer electrolytes with in-built fast interfacial transport for secondary lithium batteries. *Nat. Energy* **4**, 365–373 (2019).
183. Bouchet, R. et al. Single-ion BAB triblock copolymers as highly efficient electrolytes for lithium-metal batteries. *Nat. Mater.* **12**, 452–457 (2013).
184. Jiang, T. et al. Solvent-free synthesis of thin, flexible, nonflammable garnet-based composite solid electrolyte for all-solid-state lithium batteries. *Adv. Energy Mater.* **10**, 1903376 (2020).
185. Wang, F. et al. Progress report on phase separation in polymer solutions. *Adv. Mater.* **31**, 1806733 (2019).
186. Seo, M. & Hillmyer, M. A. Reticulated nanoporous polymers by controlled polymerization-induced microphase separation. *Science* **336**, 1422–1425 (2012).
187. Motokawa, R. et al. Photonic crystals fabricated by block copolymerization-induced microphase separation. *Macromolecules* **49**, 6041–6049 (2016).
188. Lee, K., Corrigan, N. & Boyer, C. Polymerization induced microphase separation for the fabrication of nanostructured materials. *Angew. Chem. Int. Ed.* **62**, e202307329 (2023).
189. Lee, M. J. et al. Elastomeric electrolytes for high-energy solid-state lithium batteries. *Nature* **601**, 217–222 (2022).
190. Lu, Y., Li, J., Zhao, Y. & Zhu, X. Lithium clustering during the lithiation/delithiation process in $LiFePO_4$ olivine-structured materials. *ACS Omega* **4**, 20612–20617 (2019).
191. Zhao, L., Pan, H., Hu, Y., Li, H. & Chen, L. Spinel lithium titanate ($Li_4Ti_5O_{12}$) as novel anode material for room-temperature sodium-ion battery. *Chin. Phys. B* **21**, 028201 (2012).
192. Ohzuku, T., Ueda, A. & Yamamoto, N. Zero-strain insertion material of $Li[Li_{1/3}Ti_{5/3}]O_4$ for rechargeable lithium cells. *J. Electrochem. Soc.* **142**, 1431 (1995).
193. Scharner, S., Weppner, W. & Schmid-Beurmann, P. Evidence of two-phase formation upon lithium insertion into the $Li_{1.33}Ti_{1.67}O_4$ spinel. *J. Electrochem. Soc.* **146**, 857 (1999).
194. Wagemaker, M., van Eck, E. R. H., Kentgens, A. P. M. & Mulder, F. M. Li-ion diffusion in the equilibrium nanomorphology of spinel $Li_{4+x}Ti_5O_{12}$. *J. Phys. Chem. B* **113**, 224–230 (2009).
195. Sun, Y. et al. Direct atomic-scale confirmation of three-phase storage mechanism in $Li_4Ti_5O_{12}$ anodes for room-temperature sodium-ion batteries. *Nat. Commun.* **4**, 1870 (2013).
196. Yu, X. et al. A size-dependent sodium storage mechanism in $Li_4Ti_5O_{12}$ investigated by a novel characterization technique combining in situ X-ray diffraction and chemical sodiation. *Nano Lett.* **13**, 4721–4727 (2013).
197. Natarajan, S., Subramanyan, K. & Aravindan, V. Focus on spinel $Li_4Ti_5O_{12}$ as insertion type anode for high-performance Na-ion batteries. *Small* **15**, 1904484 (2019).
198. Mu, L. et al. Revealing the chemical and structural complexity of electrochemical ion exchange in layered oxide materials. *J. Am. Chem. Soc.* **146**, 26916–26925 (2024).
199. Astles, T. et al. In-plane staging in lithium-ion intercalation of bilayer graphene. *Nat. Commun.* **15**, 6933 (2024).
200. Wang, Q. et al. Fast-charge high-voltage layered cathodes for sodium-ion batteries. *Nat. Sustain.* **7**, 338–347 (2024).
201. Van der Ven, A., Deng, Z., Banerjee, S. & Ong, S. P. Rechargeable alkali-ion battery materials: theory and computation. *Chem. Rev.* **120**, 6977–7019 (2020).
202. Poizot, P., Laruelle, S., Grugeon, S., Dupont, L. & Tarascon, J. M. Nano-sized transition-metal oxides as negative-electrode materials for lithium-ion batteries. *Nature* **407**, 496–499 (2000).
203. Li, H., Richter, G. & Maier, J. Reversible formation and decomposition of LiF clusters using transition metal fluorides as precursors and their application in rechargeable Li batteries. *Adv. Mater.* **15**, 736–739 (2003).
204. Sasaki, T., Ukyo, Y. & Novák, P. Memory effect in a lithium-ion battery. *Nat. Mater.* **12**, 569–575 (2013).
205. Madej, E., La Mantia, F., Schuhmann, W. & Ventosa, E. Impact of the specific surface area on the memory effect in Li-ion batteries: the case of anatase TiO_2. *Adv. Energy Mater.* **4**, 1400829 (2014).
206. Wagemaker, M., Kentgens, A. P. M. & Mulder, F. M. Equilibrium lithium transport between nanocrystalline phases in intercalated TiO_2 anatase. *Nature* **418**, 397–399 (2002).
207. Wagemaker, M., van Well, A. A., Kearley, G. J. & Mulder, F. M. The life and times of lithium in anatase TiO_2. *Solid State Ion.* **175**, 191–193 (2004).
208. van de Krol, R., Goossens, A. & Meulenkamp, E. A. In situ X-ray diffraction of lithium intercalation in nanostructured and thin film anatase TiO_2. *J. Electrochem. Soc.* **146**, 3150 (1999).
209. Dai, J., Li, S. F. Y., Gao, Z. & Siow, K. S. Novel method for synthesis of γ-lithium vanadium oxide as cathode materials in lithium ion batteries. *Chem. Mater.* **11**, 3086–3090 (1999).
210. Coccíantelli, J. M. et al. Electrochemical and structural characterization of lithium intercalation and deintercalation in the γ-LiV_2O_5 bronze. *Solid State Ion.* **50**, 99–105 (1992).
211. Christensen, C. K., Sørensen, D. R., Hvam, J. & Ravnsbæk, D. B. Structural evolution of disordered $Li_xV_2O_5$ bronzes in V_2O_5 cathodes for Li-ion batteries. *Chem. Mater.* **31**, 512–520 (2019).
212. Pralong, V. et al. Electrochemical synthesis of a lithium-rich rock-salt-type oxide $Li_5W_2O_7$ with reversible deintercalation properties. *Inorg. Chem.* **53**, 522–527 (2014).
213. Mikhailova, D. et al. Lithium insertion into Li_2MoO_4: reversible formation of $(Li_3Mo)O_4$ with a disordered rock-salt structure. *Chem. Mater.* **27**, 4485–4492 (2015).
214. Zhao, C. et al. Rational design of layered oxide materials for sodium-ion batteries. *Science* **370**, 708–711 (2020).
215. Wang, Q. et al. Ionic potential for battery materials. *Nat. Rev. Mater.* **10**, 697–712 (2025).
216. Wang, Q., Zhao, C. & Wagemaker, M. Rational design of layered oxide materials for batteries. *Acc. Chem. Res.* **58**, 1742–1753 (2025).
217. Mizushima, K., Jones, P. C., Wiseman, P. J. & Goodenough, J. B. Li_xCoO_2 ($0<x\leq1$): A new cathode material for batteries of high energy density. *Solid State Ion.* **3-4**, 171–174 (1981).
218. Hua, W. et al. Chemical and structural evolution during the synthesis of layered $Li(Ni,Co,Mn)O_2$ oxides. *Chem. Mater.* **32**, 4984–4997 (2020).
219. Pastor, E. et al. Complementary probes for the electrochemical interface. *Nat. Rev. Chem.* **8**, 159–178 (2024).
220. Wang, Q. et al. Grain-boundary-rich interphases for rechargeable batteries. *J. Am. Chem. Soc.* **146**, 31778–31787 (2024).
221. Wang, Q. et al. Interphase design for lithium-metal anodes. *J. Am. Chem. Soc.* **147**, 9365–9377 (2025).
222. Wang, Q. et al. Entropy-driven liquid electrolytes for lithium batteries. *Adv. Mater.* **35**, 2210677 (2023).
223. Zhang, Z. et al. Phase transformation and microstructural evolution of CuS electrodes in solid-state batteries probed by in situ 3D X-ray tomography. *Adv. Energy Mater.* **13**, 2203143 (2023).
224. Hua, W. et al. Structural insights into the formation and voltage degradation of lithium- and manganese-rich layered oxides. *Nat. Commun.* **10**, 5365 (2019).
225. Yang, F. et al. Nanoscale morphological and chemical changes of high voltage lithium–manganese rich NMC composite cathodes with cycling. *Nano Lett.* **14**, 4334–4341 (2014).
226. Xu, B., Fell, C. R., Chi, M. & Meng, Y. S. Identifying surface structural changes in layered Li-excess nickel manganese oxides in high voltage lithium ion batteries: a joint experimental and theoretical study. *Energy Environ. Sci.* **4**, 2223–2233 (2011).
227. Finegan, D. P. et al. Spatial quantification of dynamic inter and intra particle crystallographic heterogeneities within lithium ion electrodes. *Nat. Commun.* **11**, 631 (2020).
228. Xu, Y. et al. In situ visualization of state-of-charge heterogeneity within a $LiCoO_2$ particle that evolves upon cycling at different rates. *ACS Energy Lett.* **2**, 1240–1245 (2017).
229. Nedyalkov, M. et al. Structural transformation and nanoscale pulverization driven by oxygen redox: implications for Li_2RuO_3 stability in lithium-ion batteries. *J. Phys. Chem. C* **129**, 11838–11850 (2025).
230. Wu, Y. et al. Highly reversible Li_2RuO_3 cathodes in sulfide-based all solid-state lithium batteries. *Energy Environ. Sci.* **15**, 3470–3482 (2022).
231. Zhang, H. et al. Layered oxide cathodes for Li-ion batteries: oxygen loss and vacancy evolution. *Chem. Mater.* **31**, 7790–7798 (2019).
232. Hu, E. et al. Evolution of redox couples in Li- and Mn-rich cathode materials and mitigation of voltage fade by reducing oxygen release. *Nat. Energy* **3**, 690–698 (2018).
233. Csernica, P. M. et al. Persistent and partially mobile oxygen vacancies in Li-rich layered oxides. *Nat. Energy* **6**, 642–652 (2021).
234. Brow, R. et al. Mechanical pulverization of Co-free nickel-rich cathodes for improved high-voltage cycling of lithium-ion batteries. *ACS Appl. Energy Mater.* **5**, 6996–7005 (2022).
235. Wen, M., Yu, J., Wang, J., Li, S. & Zeng, Q. Electrochemical performance of Cu_6Sn_5 alloy anode materials for lithium-ion batteries fabricated by controlled electrodeposition. *RSC Adv.* **14**, 24703–24711 (2024).
236. Vema, S., Berge, A. H., Nagendran, S. & Grey, C. P. Clarifying the dopant local structure and effect on ionic conductivity in garnet solid-state electrolytes for lithium-ion batteries. *Chem. Mater.* **35**, 9632–9646 (2023).
237. Hatz, A.-K. et al. Chemical stability and ionic conductivity of LGPS-type solid electrolyte tetra-Li_7SiPS_8 after solvent treatment. *ACS Appl. Energy Mater.* **4**, 9932–9943 (2021).
238. Kam, R. L. et al. Crystal structures and phase stability of the Li_2S–P_2S_5 system from first principles. *Chem. Mater.* **35**, 9111–9126 (2023).
239. Xue, Z. et al. Asynchronous domain dynamics and equilibration in layered oxide battery cathode. *Nat. Commun.* **14**, 8394 (2023).
240. Li, J. et al. Dynamics of particle network in composite battery cathodes. *Science* **376**, 517–521 (2022).
241. Stephan, A. K. Completing the picture of the solid electrolyte interphase. *Joule* **3**, 1812–1814 (2019).
242. Jiang, Z. et al. Machine-learning-revealed statistics of the particle-carbon/binder detachment in lithium-ion battery cathodes. *Nat. Commun.* **11**, 2310 (2020).
243. Li, Z. et al. Fast kinetics of multivalent intercalation chemistry enabled by solvated magnesium-ions into self-established metallic layered materials. *Nat. Commun.* **9**, 5115 (2018).
244. McClary, S. A. et al. A heterogeneous oxide enables reversible calcium electrodeposition for a calcium battery. *ACS Energy Lett.* **7**, 2792–2800 (2022).

Acknowledgements

The authors acknowledge support from the National Nature Science Foundation of China (22579078 and 52572281), Guangdong Basic and Applied Basic Research Foundation (2026A1515012175 and 2026A1515012386), and Shenzhen Natural Science Foundation in Basic Research Fund (JCYJ20250604144220026).

Author contributions

Q.W. conceived the idea and designed the framework of the article. All authors contributed to the discussion and researched data for the manuscript. Q.W., X. Z. and C.Z. prepared and reviewed the manuscript.

Competing interests

The authors declare no competing interests.

Additional information

Peer review information *Nature Reviews Chemistry* thanks Haegyeom Kim and the other, anonymous, reviewers for their contribution to the peer review of this work.

Publisher's note Springer Nature remains neutral with regard to jurisdictional claims in published maps and institutional affiliations.

Springer Nature or its licensor (e.g. a society or other partner) holds exclusive rights to this article under a publishing agreement with the author(s) or other rightsholder(s); author self-archiving of the accepted manuscript version of this article is solely governed by the terms of such publishing agreement and applicable law.

© Springer Nature Limited 2026

[1]Shenzhen Key Lab of Energy Materials for Carbon Neutrality, Shenzhen Institutes of Advanced Technology, Chinese Academy of Sciences, Shenzhen, China. [2]Department of Mechanical and Energy Engineering, Southern University of Science and Technology, Shenzhen, China. [3]Electrical Energy Storage Technology, Technische Universität Berlin, Berlin, Germany. [4]Songshan Lake Materials Laboratory, Dongguan, China. [5]State Key Laboratory of Metal Matrix Composites, School of Materials Science and Engineering, Shanghai Jiao Tong University, Shanghai, China. [6]Department of Radiation Science and Technology, Delft University of Technology, Delft, the Netherlands. [7]Key Laboratory for Renewable Energy, Institute of Physics, Chinese Academy of Sciences, Beijing, China. [8]School of Shenzhen International Graduate, Tsinghua University, Shenzhen, China. [9]These authors contributed equally: Chenglong Zhao, Xia Zhang.